Biosensors for measuring matrix metalloproteinases: an emerging research field

Arno Kirchhain[1], Noemi Poma[1], Pietro Salvo[1,2], Lorena Tedeschi[2], Bernardo Melai[1], Federico Vivaldi[1], Andrea Bonini[1], Maria Franzini[3], Laura Caponi[3], Arianna Tavanti[4], Fabio Di Francesco[1*]

[1]Department of Chemistry and Industrial Chemistry – University of Pisa, Italy;

[2]Institute of Clinical Physiology – National Research Council, Pisa, Italy;

[3]Department of Translational Research and New Technologies in Medicine and Surgery – University of Pisa;

[4]Department of Biology – University of Pisa, Italy.

Arno Kirchhain arno.kirchhain@dcci.unipi.it; Noemi Poma vio_noemia15@hotmail.com; Pietro Salvo pietro.salvo@gmail.com; Lorena Tedeschi tedeschi@ifc.cnr.it, Bernardo Melai melai@dcci.unipi.it; Federico Vivaldi federico-vivaldi@virgilio.it; Andrea Bonini bonini-andrea@virgilio.it; Franzini maria.franzini@unipi.it; Laura Caponi laura.caponi@unipi.it; Arianna Tavanti arianna.tavanti@unipi.it;

* Corresponding author, Fabio Di Francesco fabio.difrancesco@unipi.it; +39 050 2219 308.

Abstract

Matrix metalloproteinases (MMPs) have been proposed as markers of many pathological conditions for their ability to degrade extracellular matrix components and remodel tissues. This review presents an overview of biosensors for the measurement of MMPs in serum, sputum and cell cultures. Major benefits and limitations of these technologies are discussed with respect to zymography and immunoassays, which are the reference methods to measure MMP activity and concentration. The paper also compares the analytical performances of sensors to the specific requirements for the application in clinical research, and comments on future trends in this field.

1- Introduction

Human matrix metalloproteinases (MMPs) are extracellular and membrane associated calcium-dependent and zinc-containing endopeptidases, i.e. proteolytic enzymes that break peptide bonds of nonterminal amino acids in target proteins. They have a broad proteolytic activity and participate in a variety of physiological (development, morphogenesis, angiogenesis, growth, wound healing, immune response and others) [1] and pathological (cancer, cardiovascular diseases, auto-immune disorders, osteoarthritis, chronic wounds among others) processes [2,3]. MMPs' deregulated expression has been associated to the progression/relapse or to the development of pathological conditions, prompting the use of MMPs as potential therapeutic targets and biomarkers for the inhibition and monitoring of disease progression, respectively [4].

MMPs are ubiquitous multi-domain enzymes belonging to the M10 family of the metalloprotease superfamily, with 23 MMPs identified in humans (MMP 1-3; MMP 7-17; MMP 19-21 and MMP 23-28) [5]. MMPs' structure (Figure 1) consists of a propeptide that keeps the enzyme inactive (zymogens or pro-MMPs) by obstructing the interaction between the catalytic site and substrate, through a cysteine switch [6]. The catalytic domain is characterized by the presence of a Zn-binding motif, in which the Zn ion is coordinated by three histidines and a solvent molecule bound to a glutamate followed by a linker peptide of variable lengths (hinge region) and a hemopexin-like domain [7,8].

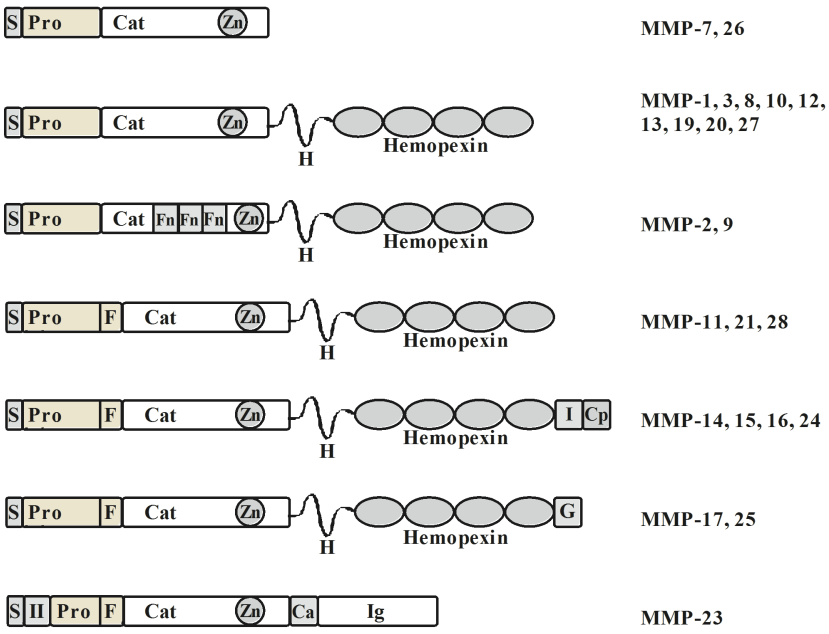

Figure 1. Multi-domain structure of human metalloproteinases (MMPs). S, signal peptide (signal anchor in MMP-23); Pro, pro-peptide; Cat, catalytic domain; Zn, Zn containing active site; H, hinge region; Fn, fibronectin insert; F, furin cleavage site; I, type I transmembrane domain; Cp, cytoplasmic domain; G, glycosylphosphatidyl inositol (GPI) anchoring domain; II, type II transmembrane domain; Ca, cysteine-rich domain; Ig, Immunoglobulin-like domain.

Besides components of the extracellular matrix (ECM), the continuous discovery of new substrates has clearly indicated that MMPs are involved in a variety of intra- and inter-cellular processes and participate in functional networks, regularly interacting with other biological molecules [9]. In addition, proteomic analysis aimed at defining MMP substrate degradomics has unveiled a plethora of new targets encompassing chemokines, cytokines, growth factors, proteases, other MMPs, MMP inhibitors, cell adhesion molecules, receptors, components of extracellular matrix and even some substrates with unknown functions, demonstrating MMPs' biological complexity and their crucial role in physiological activities [10].

The involvement of MMPs in pathological conditions has long been studied [2], and it is recognized that MMPs have pleiotropic effects, depending on the disease, the available substrate, the source and location of MMPs, and the stage of disease [10,11]. A clear example is provided by the dual tumorigenic and anti-tumorigenic role of MMPs during cancer development e.g. cancer metastasis suppression by the same protease (MMP-11), that earlier promoted tumour progression in a breast cancer cell model [12].

MMPs' physiological activities are finely tuned and coordinated by a complex regulatory network composed by tissue-inhibitors of metalloproteinases (TIMPs), MMPs, cofactors, receptors, substrates and other proteins [7]. In normal cell conditions the expression of MMPs is barely detectable, in contrast to what is observed during a state of perturbed homeostasis [13]. Several MMPs have been associated with different pathologies, where their high level of expression correlates to poor prognosis, such as MMP-21, MMP-9, whose highly expressed transcripts represent signatures for specific types of cancer [14]. Nevertheless, over expression of MMPs in a given pathology does not necessarily reflect a progression of the disease, since it is now accepted that MMPs may also have a protective effect e.g. type MMP-8, whose over-expression is related to a reduced metastatic potential in breast cancer [15].

Overall, the current knowledge of MMPs provides a perception of their multifunctional implication in biological and pathological processes, highlighting their relevance as potential therapeutic options. A better understanding of which MMP is actually involved (and when) in a specific pathological process could lead to the potential application of MMPs as biomarkers for early diagnostic approaches and for estimating the prognosis of the disease. Over the last decade, the growing interest for MMPs has pushed the development of a variety of devices bases on different recognitions methods and signal transductions aimed at measuring MMP enzymatic activity.

This manuscript provides an updated overview of the latest MMP sensor technologies pointing out their strengths and weaknesses compared to current techniques measuring MMPs. Technological implementation of current sensing devices are discussed as well as their potential applications in the clinical settings for a timely and effective monitoring of patient outcome.

2- Current measurement techniques

Assays based on the hydrolysis of proteic or fluorogenic peptide substrates and enzymatic immunoassays are the most widely used methods to measure MMPs activities in clinical laboratories [16,17]. MMPs are typically measured in serum, but sputum has been analysed in patients suffering from pulmonary diseases (e.g. chronic obstructive pulmonary disease, COPD) and synovial cell cultures in the case of

osteoarthritis. Concentrations in these biofluids of most relevant MMPs in healthy subjects and in patients suffering from different diseases are reported in Table 1. It is noteworthy that different measurement techniques provide significantly different ranges of analytes both in patients and healthy controls. The spread of values in healthy subjects from different studies seems larger than the differences between patients and controls in a same study. This is particularly evident with results obtained with different immunoassays.

2.1 Zymography

Zymography is an electrophoretic technique in which a sample is separated in denaturing, non-reducing conditions. The separation is performed on a substrate (collagen, gelatine, etc.) containing polyacrylamide gel. Upon renaturation of the enzyme, via change of detergent from SDS to Triton-X, the enzyme digests the substrate [18]. Proteolytic activity can be detected as clear bands of the Coomassie stained substrate; intensity can be measured by densitometry so that a semi-quantitative evaluation can be obtained by dedicated calibration curves.

Gel zymography also allows the separation of different forms of the same MMP such as the free active MMP, the proactive form (not cleaved, the zymogen), a homodimer or complexes with other proteins. However, the use of SDS may result in an inaccurate evaluation of the real biological activity in the sample. In fact, this surfactant promotes the separation of active MMPs from non-covalently bound TIMPs and the denaturation also unfolds the pro-enzyme, unlocking the catalytic site and allowing an active conformation that can persist even after a partial renaturation [19]. Nonetheless, gel zymography has been considered for a long time the gold standard to measure MMPs activities, because it is quite simple and sensitive.

Table 1. Functional properties and approximated concentrations of selected human matrix metalloproteinases in healthy subjects and in patients with different diseases.

MMP	Accession number	Function[a]	Disease	Serum Concentration		Other body fluid concentration	References
				Healthy	Disease		
1	P03956	Cleaves collagen (type I, II, III, VII and X).	Acute viral hepatitis	122±18 ng/mL[b]	76±12 ng/mL[b]		[20]
			Dilated cardiomyopathy	2.4±0.4 ng/mL[c]	6.0±0.9 ng/mL[c]		[21]
			Osteoarthritis of the hip	2.2–23 ng/mL[d]	15.5±9.7 ng/mL (1.8-36.9 ng/mL[g])[d]	Synovial cell cultures: 33±41 ng/mL (3.5-183 ng/mL[g])[d]	[22]
			Rapidly destructive osteoarthritis of the hip		17±11 ng/mL (3.4-42.5 ng/mL[g])[d]	Synovial cell cultures: 351±538 ng/mL (23.5-1850 ng/mL[g])[d]	
2	P08253	Participates in vascular remodelling, angiogenesis, tissue repair, tumour invasion, inflammation, and atherosclerotic plaque rupture. Degrades extracellular matrix proteins and several non-matrix proteins such as big endothelial 1 and beta-type CGRP, promoting vasoconstriction. Cleaves KISS at a Glycine-/-Leucine bond. Potential role in myocardial cell death pathways. Contributes to myocardial oxidative stress by regulating the activity of GSK3beta. Cleaves GSK3beta in vitro. Involved in the formation of the fibrovascular tissues in association with MMP14.	Acute viral hepatitis	1555±133 ng/mL[b] (425±14 ng/mL[e])	790±68 ng/mL[b] 261±14 ng/mL[e]		[20]
			Cystic fibrosis associated to pulmonary exacerbation (PEx)	280 ng/mL[b]	NoPEx: 202 ng/mL PEx: 168 ng/mL[b]		[23]
			Colorectal cancer	235 (108–384[g]) ng/mL[b]	180 (87–476[g]) ng/mL[b]		[24]
			Colorectal cancer			Normal mucosa of colorectal cancer patients: 4.8 (0–30.5[g]) ng/mg. Median carcinomas 10.6 ng/mg[b]	[25]
			Osteoarthritis of the hip	367–770 ng/mL[d]	593±119 ng/mL (409-848 ng/mL[g])[d]	Synovial cells: 314±166 ng/mL; (91-676ng/mL[g])[d]	[22]
			Rapidly destructive osteoarthritis of the hip		630±202 ng/mL (415-1150 ng/mL[g])[d]	Synovial cells: 563±443ng/mL; (63-1670 ng/mL[g])[d]	
3	P08254	Degrades fibronectin, laminin, gelatins (type I, III, IV, and V), collagens (type III, IV, X, and IX) and cartilage proteoglycans. Activates	Acute viral hepatitis	21±5 ng/mL[b]	5±3 ng/mL[b]		[20]
			Osteoarthritis of the hip	15–72 ng/mL[d]	41±28 ng/mL (12.6-112 ng/mL[g])[d]	Synovial cells:23± 32 ng/mL; (12.5-147 ng/mL[g])[d]	[22]

		procollagenase.	Rapidly destructive osteoarthritis of the hip		100±63 ng/mL (15.1-223 ng/mL[g])[d]	Synovial cells:114±176 ng/mL; (12.5-636 ng/mL[g])[d]	
			Rheumatoid arthritis (RA)	Men: 65 ±29 ng/mL Women: 29 ± 13 ng/mL[d]	Early RA: 246 ± 268 ng/mL Late RA: 225 ±237 ng/mL[d]		[26]
7	P09237	Degrades casein, gelatins (type I, III, IV, and V) and fibronectin. Activates procollagenase.	Idiopathic pulmonary fibrosis (IPF)			(Sputum) Healthy 20 (2-93[g]) ng/mL; IPF 46 (0.008-190[g]) ng/mL[b]	[27]
			Chronic obstructive pulmonary disease (COPD)			(Sputum) Healthy 20 (2-93[g]) ng/mL; COPD 17 (3-195[g]) ng/mL[b]	
8	P22894	Degrades fibrillar type I, II, and III collagen.	Colorectal cancer	17 ng/mL[f]	53 ng/mL[f]		[28]
			Cystic fibrosis associated to pulmonary exacerbation (PEx)	17 ng/mL[b]	NoPEx: 37 ng/mL PEx: 62 ng/mL[b]		[23]
9	P14780	Cleaves type IV and type V collagen into large C-terminal three quarter fragments and shorter N-terminal one quarter fragments. Degrades fibronectin but not laminin or Pz-peptide. May play an essential role in local proteolysis of the extracellular matrix and in leukocyte migration. Potential role in bone osteoclastic resorption. Cleaves KISS1 at a Glycine-/-Leucine bond.	Acute viral hepatitis	65±9 ng/mL[b]; 5.8 ± 0.3 ng/mL[e]	34±7 ng/mL[b]; 2.7±0.2 ng/mL[e]		[20]
			Duchenne muscular dystrophy	73 ng/mL[b]	1185 ng/mL[b]		[29]
			Chronic obstructive pulmonary disease (COPD)			(Sputum) Healthy 70 (10–471[g]) ng/mL; COPD 264 (31–969[g]) ng/mL[b]	[27]
			Colorectal cancer			Normal mucosa of colorectal cancer patients: 3.2 (0.2–164.7[g]) ng/mg protein. Median carcinomas 36.7 ng/mg protein[b]	[25]
			Cystic fibrosis associated to pulmonary exacerbation (PEx)	346 ng/mL[b]	NoPEx: 486 ng/mL PEx: 792 ng/mL[b]		[23]
			Idiopathic pulmonary fibrosis (IPF)			(Sputum) Healthy 70 (10-471[g]) ng/mL; IPF 415 (18-970[g]) ng/mL;	[27]

			Osteoarthritis of the hip	12–71 ng/mL[d]	41±14 ng/mL (25-79.9 ng/mL[g])[d]	Synovial cells: 3.11±0.02 ng/mL; (3.1-3.2 ng/mL[g])[d]	[22]
			Rapidly destructive osteoarthritis of the hip		191±188 ng/mL (28.5-747 ng/mL[g])[d]	Synovial cells: 11±9 ng/mL; (3.1-30.5 ng/mL[g])[d]	
14	P50281	Degrades various components of the extracellular matrix such as collagen. Activates progelatinase A. Essential for pericellular collagenolysis and modelling of skeletal and extraskeletal connective tissues during development. May be involved in actin cytoskeleton reorganization by cleaving PTK7. Acts as a positive regulator of cell growth and migration via activation of MMP-15. Involved in the formation of the fibrovascular tissues in association with pro-MMP2. Cleaves ADGRB1 to release vasculostatin-40 which inhibits angiogenesis.	Invasive ductal breast cancer	9±2 ng/mL[b]	17±6 ng/mL[b]		[30]

[a]www.uniprot.org, CGRP, calcitonin gene-related peptide; KISS, Kinase Substrate Sensor; GSK3B, Glycogen synthase kinase 3 beta; PTK7, protein tyrosine kinase; ADGRB1, adhesion G protein-coupled receptor B1

[b]Measurement by enzyme-linked immunosorbent assay (ELISA)

[c]Measurement by two-step sandwich enzyme immunoassay (EIA)

[d]Measurement by one-step sandwich enzyme immunoassay (EIA)

[e]Measurement by zymography

[f]Time-resolved immunofluorometric assay (IFMA)

[g]Range of measurement values

Among gel zymographies, gelatine zymography aimed at measuring MMP-2 and MMP-9 activity is the most consolidated; casein is the preferred substrate for MMP-3 and MMP-10 (stromelysins), whereas collagen is used for MMP-1 and MMP-13 activity (collagenases). No ideal substrates have been found to measure the activity of other MMPs. Methods involving the hydrolysis of natural protein substrates (labelled or not), including zymography, have been thoroughly reviewed by Lombard et al. [16]. Variations of the conventional gel zymography to improve the basic technique have also been developed [31].

2.2 Immunoassays

MMPs antibodies became available in the ’90s, offering the specificity needed for an unequivocal identification and the flexibility for use in a variety of assays. Enzyme-linked immunosorbent assays (ELISAs) are extremely popular methods based on the interaction of a target molecule (antigen) with its specific antibody that can be used to quantify the amount of a protein in a sample. MMP detection is achieved by the adsorption of enzymes from the sample to the bottom of a microliter plate (direct ELISA) or by the use of a primary capture antibody (sandwich ELISA), followed in both cases by the addition of an anti-MMP antibody conjugated with a chromogenic enzyme [17]. The chromogenic enzyme converts a substrate into a coloured or fluorescent chemical and allows the quantification of a specific MMP via UV-vis absorption or fluorescence measurements with detection limits in the range 0.01-10 ng [17]. The capture antibody and the detecting antibody bind different epitopes of the same MMP. Washing at each step helps removing unwanted contaminants from the sample.

3- Sensing technologies

A biosensor is a self-contained device combining a receptor or Bio-Recognition Element (BRE), capable of a selective interaction with an analyte, and a transducer, signalling the occurrence of the receptor-analyte interaction [32]. Since MMPs are proteins with enzymatic activity, recognition can happen by exploiting their affinity for a receptor, their catalytic activity or combining both strategies [16,17]. The term “sensor” is sometimes misused in literature to describe BREs whose interaction with the analyte is revealed by a benchtop instrument (e.g. a fluorimeter or a microscope) instead of a self-contained transducer. In this paper, we identify these systems as molecular probes, and describe them in a separate paragraph before the “true” sensors.

3.1 Molecular probes

An effective molecular probe combines in a molecule or in a supramolecular structure an "interacting moiety" and a "detectable moiety". The former is necessary to bind a specific analyte, whereas the latter allows detection by the selected technique (e.g. optical, radioactive, and mass spectrometric) once the probe has bound the target. Activity based probes and Fluorescence Resonance Energy Transfer (FRET) based probes are mostly used to assess MMPs' activity, while labelled antibodies are used to detect the MMPs' presence. The antibody detects the protein whether it is active or not, but only the active form can cleave probes or substrates. For this reason, data obtained with these two approaches can differ if inactive forms of the protein are present in the sample (e.g. zymogen).

3.1.1 Activity based probes

Activity Based Probes (ABPs) bind the MMPs' active sites where the proteolytic activity of the enzymes takes place. ABPs typically combine three elements: 1) a reactive group that covalently binds the probe to the enzyme active site; 2) a linker, such as a peptide sequence, used to improve the specificity of the probe and/or to connect the reactive group to the tag; 3) a tag, such as a fluorophore, which labels the enzyme and allows its detection and/or purification [33]. ABPs allow the generation of snapshot "images" of the target presence and distribution, but they cannot monitor dynamic processes, as the covalent labelling destroys the enzyme activity upon binding.

An attempt to design an ABP library for MMPs was reported by Sieber et al. [34]. The ABPs included inhibitors of the MMPs activity, benzophenone as photo-cross-linker and rhodamine as tag. The authors modified the MMP substrates (e.g. Marimastat) by adding a moiety (benzophenone) able to be photoactivated by UV light to covalently bind to MMP and a tag moiety (rhodamine) that, attached to the MMP, revealed the binding of the substrate with the molecule's active site [35]. However, these ABPs could not cover the whole metalloprotease superfamily due to the large variety of active site structures amongst different MMPs. Nury et al. modified the scaffold of a phosphinic peptide, a broad-spectrum MMP-inhibitor, and designed a probe to radio-image MMP□2, □3, □8, □9, □12, □13 and □14 in biological fluids or tissue extracts [36]. This probe, which showed a nanomolar affinity towards MMPs, included a photolabile diazirine group to crosslink to the MMPs active sites and a radioactive label (2-3 [^{3}H]propionic acid moiety) for detection.

3.1.2 Substrate Based Probes

If the probe–target interaction is revealed by changes in the probe structure leaving the target MMP unaffected, then the proteolytic activity can be monitored over time and often the signal is enhanced by the accumulation of "detectable" products.

Optical detection, in particular fluorescence based methods, is mainly used for this substrate cleavage approach [37]. MMPs activities can be quantified by measuring changes: 1) in the fluorescence signal from a pair of dyes that interact via resonance energy transfer [38]; 2) in the fluorescence intensity upon the presence or absence of an MMP inhibitor [39,40]; 3) in the fluorescence polarization [41]. Knapinska et al. reviewed probes with small fluorophores and quenching groups synthesized for the detection of MMPs [42]. A triple-helical peptide (THP) was used for an in-vivo imaging of MMP-2 and MMP-9 in a tumour animal model [43]. This THP included a modified type V collagen sequence that was hydrolysed mainly by MMP-2 and MMP-9. A molecular probe was then synthesized by covalently conjugating near-infrared fluorescent dyes (LS276) close to the hydrolysis site. The close proximity of the dyes made them relatively non-fluorescent within the probe; however, when the THP was cleaved from the MMPs, six labelled peptide chains were released, thus enhancing the fluorescence. Quantum dots [44,45] and other nanoparticles/nanostructures can also be used as fluorophores or quenchers, as recently reviewed [46].

Song et al. utilized the fluorescence quenching capability of a graphene oxide surface functionalized with a fluorescein isothiocyanate (FITC) labelled peptide to assess MMP-2 activity. The hydrolytic action of MMP-2 cleaved the peptide, thus restoring the FITC fluorescence. This biosensor achieved a LOD of 2.5 ng/mL and proved to be highly specific for MMP-2 when tested against a series of interferents (amongst others MMP-1/9/13). Further tests in diluted human serum demonstrated its sensing capabilities in complex matrixes [47].

As fluorescent probes suffer from photo-bleaching, auto-fluorescence and can induce cytotoxic reactions in biological media, bioluminescent probes can be a better alternative since auto-fluorescence is absent and background noise is low. Bioluminescence is the emission of light in living organisms produced by the oxidation of a molecule catalysed by an enzyme, typically luciferin and luciferase, respectively. Kim et al. conjugated gold nanoparticles to a mutant Renilla luciferase (Luc8) and showed that bioluminescence increased 15-fold over background emission when MMP-2 was present [48]. Yao et al. genetically fused a peptide containing an amino sequence of Pro-Leu-Gly-Val-Arg-NH_2 (PLGVR) and a six□histidine (6 x His) tag to Luc8 [49]. In the presence of Ni^{2+}, the carboxylic acids on the quantum dot (QD) surface formed complexes with the 6 x His tag and induced light emission from the QDs by bioluminescence resonance energy transfer (BRET). When MMP-2 cleaved PLGVR, BRET decreased permitting the MMP-2 detection at a concentration of 2 ng/mL. An in-vivo

bioluminescent probe for the detection of MMP-2 and MMP-9 activity was reported by Xia et al., who injected ^{64}Cu-labeled collagen-binding quinolyl luciferin (CB-qLuc) in tumour-bearing mice [50].

3.1.3 Antibodies and other affinity-based probes

Several assays (single or multiplexed) are available based on labelled antibodies as molecular probes. Antibody-coated CdSe/CdS/ZnS quantum dots (Ab-QDs) were sprayed on colon tumour tissues and the residual fluorescence of Ab-QDs after washing allowed the imaging of MMP-9 and MMP-14 [51], whereas an MMP-9 antibody labelled with technetium-99m (Tc-McAb) was used for the non-invasive detection of MMP-9 activity in-vivo [52].

Although the most popular BREs are protein-based, oligonucleotide probes directly interacting with the target molecule were recently explored. Aptamers (from Latin *aptus*= able to) are short nucleotide sequences or peptide molecules empirically selected in vitro from large libraries of random sequences on the basis of their ability to selectively bind a target molecule thanks to their intramolecular folding and 3D structure [53]. Da Rocha Gomes et al. proposed a technetium-99m mercaptoacetyltriglycine (^{99m}Tc-MAG3) aptamer to detect hMMP-9 in slices of human brain tumours [54], whereas Kryza used three derivatives of a modified RNA aptamer (F3B) to detect hMMP-9 in melanomas and found that protease was overexpressed in the presence of metastases [55].

3.2 Sensors

In this section on sensing methodologies and concepts, sensors used for the detection of MMPs are classified in four groups: electrochemical sensors, surface plasmon resonance (SPR) based sensors, other optical sensors and less common sensing techniques.

3.2.1 Electrochemical sensors

All classical electrochemical sensing techniques have been used for MMP detection, but voltammetry is certainly the most popular (Table 2).

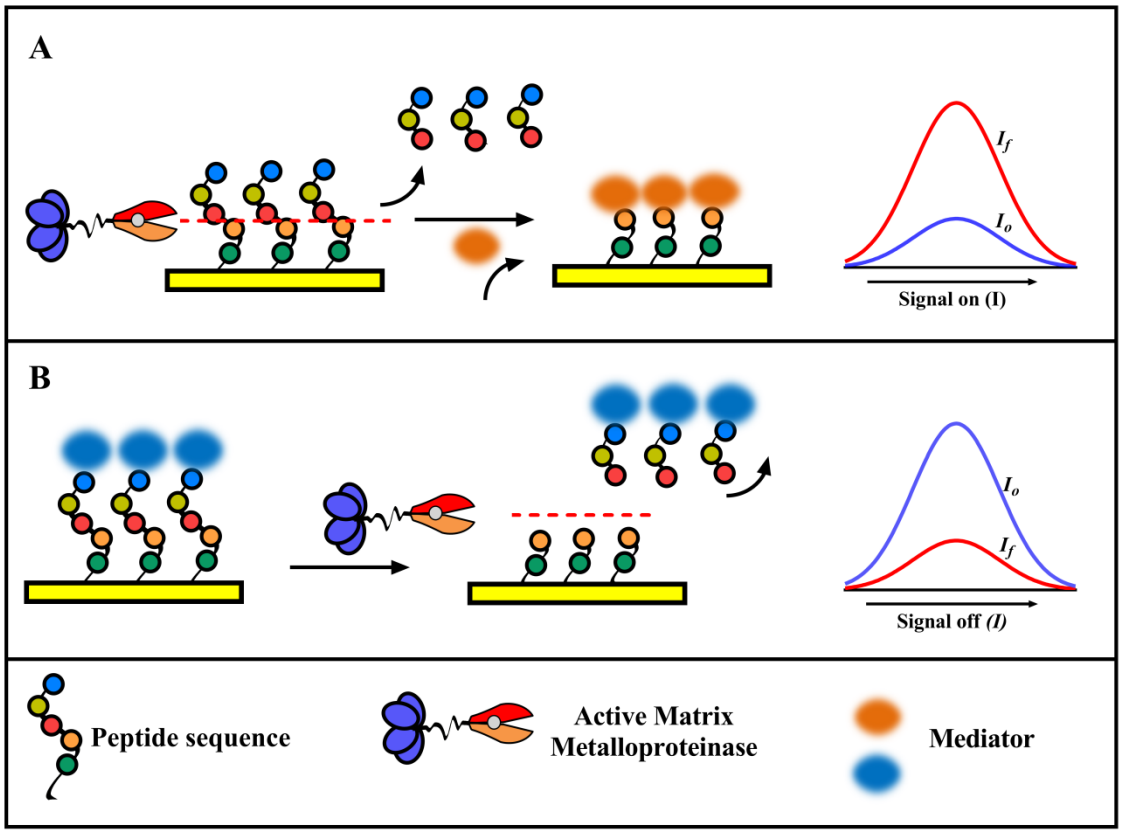

Figure 2. General principle of turn-on and turn off strategy. A) Turn-on probes: the proteolytic interaction produces free sites for the attachment of the redox mediator and the signal intensity increases. B) Turn-off probes: redox mediators are removed from the sensor surface by the enzymatic activity and the signal intensity decreases.

In a voltammetric biosensor, the potential between a functionalized working electrode and a reference electrode is varied and the current between an auxiliary electrode and working electrode is recorded [56]. These sensors follow either a turn-on or a turn-off strategy (Figure 2). In the turn-on approach, the working electrode is functionalized with specific peptide sequences that are selectively hydrolysed by the target MMP, thus making the electrode surface accessible to redox mediators (Figure 2A). The voltammetric response is generated from the redox reactions of the mediator and is proportional to the accessible electrode surface. In a turn-off approach (Figure 2B), the working electrode is functionalized with enzyme-specific peptide sequences containing or interacting with a redox mediator. In this case, the hydrolysis of peptides removes the mediator from the electrode and decreases the response.

Xu et al. implemented nanomaterials for the detection of MMP-2 with a turn-on approach [57]. First, a glassy carbon electrode (GCE) was modified with gold nanoparticles functionalized with an MMP-2 specific peptide layer labelled with biotin tags. The sensor was then incubated with buffer solutions containing MMP-2. After the hydrolysis of peptides, the biotin tags remaining on the

surface were used to attach redox active CeO_2 nanospheres loaded with Pt/Pd nanoparticles and streptavidin linkers. The decomposition of H_2O_2 by the Pt/Pd nanoparticles was finally monitored by differential pulse voltammetry (DPV), a technique in which regular voltage pulses are superimposed to linear sweeps of potential and the current difference at each potential change is plotted against potential. A LOD equal to 0.078 pg/mL was assessed in phosphate buffer solutions (PBS) with MMP-2 concentrations in the range 0.1 pg/mL - 10 ng/mL. Such low LOD is the combined result of the turn-on approach and DPV. The turn-on approach has a negligible background noise, whereas the DPV removes the charging current from the voltammetric peak.

Wang et al. described the development of a DPV-based sensor combining peptide cleavage and DNA amplification [58]. A peptide sequence specific to MMP-2 was conjugated onto magnetic polystyrene microspheres (PSC) that were further modified with Au-NPs linked to a DNA fragment (AuNP-DNA_1). The MMP-2 action released the AuNP-DNA_1 sequence which was then used to form a duplex DNA with complementary DNA fragments labelled with methylene-blue (MB-DNA_2). Application of an exonuclease hydrolysed the DNA fragment and liberated the methylene blue redox mediator. The redox mediator was then recognized by curcurbit[7]uril structures on the electrode surface leading to an increase in the DPV signal. A LOD of 0.15 pg/mL and a linear range from 0.5 pg/mL to 50 ng/mL were reported.

Turn-off probes with ferrocene [59,60], thionine [61] and methylene blue [62] as redox mediators conjugated to peptides allowed to achieve detection limits in the pg/mL range (Table 2). In order to monitor the metabolism of cell cultures, Shin et al. embedded a voltammetric sensor functionalized with an MMP-9 specific peptide sequence in a microfluidic reactor containing an U-937 cell culture [63]. Addition of phorbol 12-myristate 13-acetate stimulated the production of MMP-9, then cleavage of the peptide released the redox mediator (MB) and decreased the square wave voltammetric (SWV) signal.

Alike ELISA assays, sandwich approaches with a capture antibody deposited on the sensor surface have been reported [64,65]. Herein a capture antibody is deposited on the sensor surface and after incubation with the analyte a second antibody binding to a different epitope is introduced. The second (detection) antibody bears the element of signal transduction (fluorescent, electrocatalytic, etc.). Yang et al. detected MMP-2 with an immunosensor using a sandwich approach [64]. MMP-2 capture antibodies were immobilized onto gold nanoparticles (Au-NPs) attached to nitrogen-doped graphene (NG) sheets that were deposited on a glassy carbon electrode. After incubation with a sample containing MMP-2, the electrode was further incubated with a bioconjugate consisting of graphene oxide whose surface had been modified with polydopamine to improve the adhesion of anti-MMP-2 labelled with horseradish peroxidase. DPV performed in PBS with the addition of

thionine and H_2O_2 produced a linear output signal between 0.0005 and 50 ng/mL, with an LOD of 0.11 pg/mL. Shi et al. adopted a similar strategy using a screen printed carbon electrode coated with graphene nanoribbons and functionalized with anti-MMP-9 antibodies [65]. After incubation with MMP-9, polystyrene microspheres (200 nm) with a polydopamine shell including Cd^{2+} and modified with an MMP-9 secondary antibody were added. The Cd^{2+}oxidation peak at -0.7 V vs Ag/AgCl in SWV was taken as the quantitative response to the concentration of MMP-9, with a linear range of 10 fg – 1 μg/mL and an LOD of 5 fg/mL.

In single-potential amperometric enzymatic biosensors, an enzyme reduces or oxidizes a co-reagent and the reaction product is detected by a further electrochemical reaction occurring on the electrode surface at constant potential. Munge et al. developed a single-potential amperometric enzymatic biosensor for the detection of MMP-3 [66]. Primary anti MMP-3 antibodies were attached to components of a single-wall carbon nanotubes "forest" protruding from pyrolytic graphite disks coated with a thin Nafion layer. After incubation with undiluted calf serum containing MMP-3, the sensor surface was further incubated with a biotinylated secondary anti-MMP-3 antibody and then with streptavidin modified HRP or secondary antibody–HRP polystyrene bead bioconjugates. An LOD was 4 pg/mL was obtained by rotating disk amperometry performed in an electrochemical cell (EC) at constant potential with hydroquinone as redox mediator.

Electrochemical impedance spectroscopy (EIS) monitors the response of an electrochemical cell to minimal perturbations of its equilibrium caused by a small amplitude alternating voltage superimposed on a DC voltage [67]. Complex impedance, including the resistance to current flow and phase shift between voltage and current, is evaluated in a broad range of frequencies by modelling the EC with an equivalent electrical circuit whose passive components describe the physical and chemical processes in action. Most impedimetric measurements are performed by first incubating the sensor with the sample and then measuring the impedance towards charge-transfer in a second solution containing a redox mediator. In 2012, Ciani et al. reported an impedimetric detection system for three wound biomarkers including MMP-9 [68]. The paper described the use of a bi-functional linker to fabricate a self-assembled-monolayer (SAM) of MMP-antibodies on a screen printed electrode. Sensor impedance was measured 20min after casting a mock wound fluid drop on the sensor. Biela et al. compared the performance for MMP-9 detection of interdigitated gold electrodes (IDEs) produced by screen printing and other microfabrication techniques [69]. Surfaces were first coated with oxidized dextran and cross-linked with MMP specific peptides. The sensing scheme included the cleavage of MMP-specific peptide sequences bound to the dextran

layer under impedance monitoring. An 18% increase of impedance was observed with screen printed electrodes after 20 min in a 200 ng/ml MMP-9 buffer solution, whereas impedance decreased by 38% after 10 min in the same solution for the microfabricated electrodes. The authors supposed that the different response depended on the stability of the dextran layer, which dissolved over time because of low adhesion on the smooth microfabricated IDEs, whereas the rough gold layer of screen-printed IDEs provided better adhesion. Tran et al. described a capacitive biosensor to assess the MMP-9 production from cells [70]. The biosensor consisted of two interdigitated microelectrode arrays housed in a fluidic chamber. The first array detected the changes in the morphology caused by the activation of MCF-7 breast cancer cells with phorbol12-myristate 13-acetate via an Electric Cell-substrate Impedance Sensing (ECIS) [71]. The change in capacitance of the second array, modified with a MMP-9-specific peptide, quantified the MMP-9 concentration. This biosensor had an LOD of 10 pM and could estimate the production of MMP-9 from living cells.

Table 2: Analytical figures of merit relevant to electrochemical sensors measuring MMPs. (DPV: Differential Pulse Voltammetry, SWV: Square Wave Voltammetry, CV: Cyclic Voltammetry, NA: not available)

Target	Reference	Year	Recognition	Signal transduction	Linear range	LOD	Sensor response	Test solution	Additional Information
MMP-2	Yang et al. [64]	2013	Antibody	DPV	0.5 pg/mL-50 ng/mL	0.11 pg/mL	$\Delta I(\mu A) = 4.20 \cdot \log(C_{MMP}) + 19.7$	PBS	r=0.997 Sensor: RSD = 6.3% (n=5); Fabrication: RSD = 5.7% (n=5)
	Jing et al. [61]	2015	Peptide cleavage	DPV	1 pg/mL-10 ng/mL	0.32 pg/mL	$\Delta I(\mu A) = 8.05 \cdot \log(C_{MMP}) + 4.87$	PBS	r =0.995 Fabrication: RSD = 6.3% (n= 6)
	Xu et al. [60]	2015	Peptide cleavage	DPV	100 pg/mL-200 ng/mL	0.2 ng/mL	$\Delta I(\mu A) = 1.24 \cdot \log(C_{MMP}) + 1.17$	Diluted human serum	r=0.993 Sensor: RSD = <5% (n=3) Fabrication: RSD = 6.5% (n=5)
	Wang et al. [58]	2016	Peptide cleavage	DPV	0.5 pg/mL -50 ng/mL	0.15 pg/mL	$\Delta I(nA) = -227 \cdot \log(C_{MMP}) - 4276.8$	Diluted human serum	r = 0.998 Fabrication: RSD = 5.90% (n=4)
	Xu et al. [57]	2016	Peptide cleavage	DPV	0.1 pg/mL-10 ng/mL	0.08 pg/mL	$I(\mu A) = 3.408 \cdot \log(C_{MMP}) - 21.31$	Diluted human serum	r = 0.997 Fabrication: RSD = 6.8% (n=6)
MMP-3	Munge et al. [66]	2010	Antibody	Single potential Amperometry	4-300 pg/mL	4 pg/mL	$I(nA) = 4.25 \cdot \log(C_{MMP}) + 0.69$	Undiluted calf serum	r =0.951 Fabrication: RSD = 10% (n = NA)
MMP-7	Liu et al. [59]	2006	Peptide cleavage	SWV	0.1-10 ng/mL	0.07ng/mL[a] (3.4 pM)	NA	Tricine Buffer	Sensor: RSD: 3.2% (n=6) Fabrication: RSD = 2.1% (n=6)
MMP-9	Ciani et al. [68]	2012	Antibody	Impedimetric	NA	100 ng/mL	NA	Mock wound fluid	NA
	Shin et al. [63]	2012	Peptide cleavage	SWV	5.58 ng/mL- 4.65 µg/mL (60 pM-50 nM)[a]	5.58 ng/mL (60 pM)[a]	NA	Cell culture/PBS buffer	0.65 pg MMP-9 $cell^{-1}$ h^{-1}(U937 cells)
	Shi et al. [65]	2014	Antibody	SWV	10 fg– 1 µg/mL	5 fg/mL	$\Delta I(\mu A) = 17.3 \cdot \log(C_{MMP}) + 345.42$	PBS	r=0.997
	Biela at al. [69]	2015	Peptide cleavage	Impedimetric	50-400 ng/mL	15 ng/mL	$\Delta Z(\%) = 0.08 \cdot (C_{MMP}) - 0.137$ (20min)	Tris Buffer	R^2=0.998
	Tran et al. [70]	2016	Peptide cleavage	Capacitive	0.93 ng/mL-0.93 µg/mL (10 pM-10 nM)[a]	0.93 ng/mL (10 pM)[a]	NA	MCF-7 cells in PBS buffer	NA

[a] Values converted from concentrations according to producer specifications

3.2.2 Surface plasmon resonance based sensors

A surface plasmon resonance (SPR) setup usually includes a prism coupling the electromagnetic wave of an incident light beam to the surface plasma polaritons generated at a gold/sensing layer interface. The selective adsorption of molecules changes the refractive index of the sensing layer and can be monitored through measurements of either angle, intensity or resonance wavelength of the reflected beam. SPR is a popular, label-free methodology (no further labelling or chemical reaction needed to monitor the binding event) widely used to determine analytes in biological matrices and has been amply reviewed [72–74].

Different methodologies and geometries have been used to fabricate SPR based sensors, such as the classical Kretschmann cell [75–77], fibre-optic biosensors [78], surface plasmon resonance imaging (SPRI) [79,80] as well as coupling of different resonance modes in a Fano resonance occurring in gold nanoslits [81] (Figure 3). The main characteristics of these sensors are summarized in Table 3.

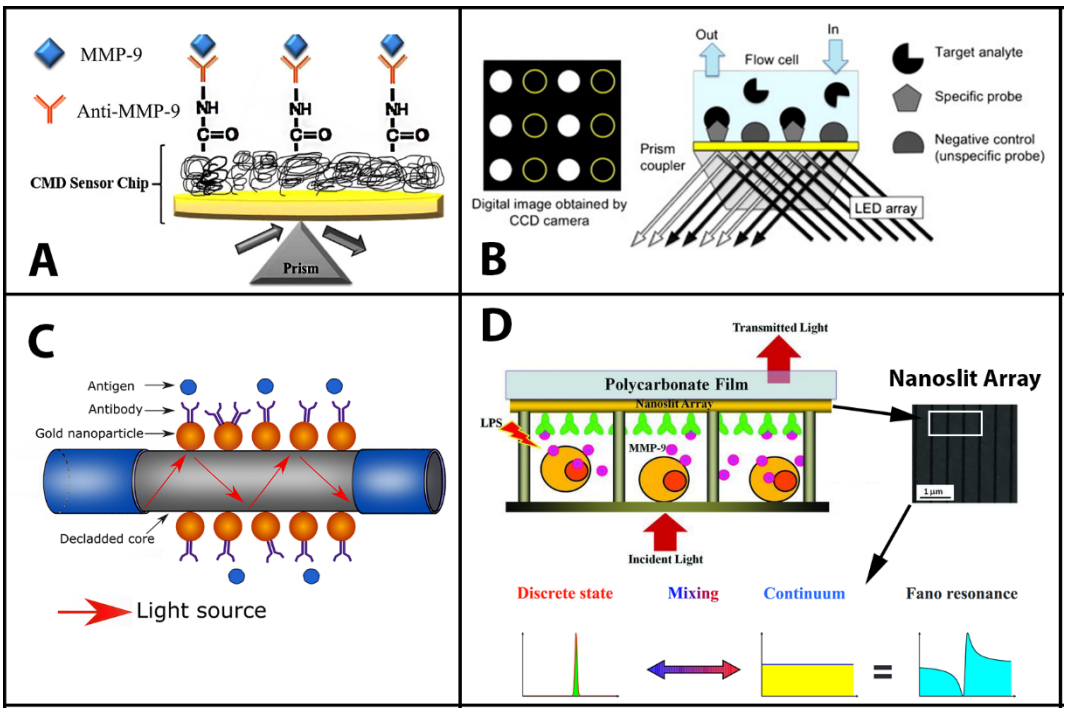

Figure 3 SPR based techniques in biosensors:

(A): Sensor chip using Kretschmann geometry covered with carboxymethyldextran (CMD) conjugated with anti-MMP-9 antibodies to measure MMP-9 concentration in diluted saliva samples [76]. (Reprinted from Biosens. Bioelectron. 81, Mohseni et al., Development of a label-free SPR sensor for detection of matrixmetalloproteinase-9 by antibody immobilization on carboxymethyldextran chip, 510-516, 2016, with permission from Elsevier.)

(B) SPR imaging chip for the parallel detection in real time of different functionalities [82]. (Reprinted from Biosens. Bioelectron., 25(5), Scarano et al., Surface plasmon resonance imaging for affinity-based biosensors, 957-966, 2010, with permission from Elsevier.)

(C) Binding of antigens to antibodies of a functionalized optic fibre resulting in enhanced absorbance of the sensing layer and reduced transmission of light [78].

(D) Experimental setup for the label-free detection of cell secretion according to [81] (Reprinted from Small, 9, Wu et al, Optofluidic platform for real-time monitoring of live cell secretory activities using Fano resonance in gold nanoslits, 3532-3540, 2013, with permission from John Wiley and Sons) and depiction of the Fano resonance as a superposition of discrete and continuous resonance modes of nanopatterned surfaces [83]. (Reprinted figure with permission from Miroshnichenko et al., Rev. Mod. Phys., 82, 2257-2298, 2010. Copyright (2010) American Physical Society).

In 2004, Pieper-Fürst et al. proposed an SPR biosensor for detecting MMP-2 with an LOD of 0.5 pM [75]. Tissue inhibitors of metalloprotease (TIMPs) were deposited on a gold electrode coated with a carboxymethyl dextranlayer. MMP-2 were captured from gold nanocolloids modified with anti-MMP-2 antibodies and then these particles formed a sandwich complex on the electrode surface thanks to the TIMP-MMP-2 binding. Mohseni et al. recently developed a carboxymethyldextran hydrogel sensor for saliva analysis [76]. After the activation of carboxymethyldextran, MMP-9 antibodies were anchored to the surface via amine coupling. The LOD was 8 pg/mL in tenfold-diluted saliva samples of patients with chronic periodontitis (Figure 3A). Yang and co-workers developed an optical sensor for the detection of membrane-bound type I MMP (MT1-MMP) for the characterization of invasive cancer cells [77]. Gold nanorods were anchored onto a glass slide and functionalized with an MMP specific peptide. Cleavage of the peptide by enzyme shifted the maximum absorption frequency of the gold rods and allowed to measure the concentrations between 1 and 100 nM.

SPRI sensors are based on the measurement of the reflectivity of p-polarized monochromatic light at fixed angle. The interaction of an analyte with the sensor surface results in a shift of the surface plasmon resonance angle and hence a variation of the surface reflectivity. The variation of the reflected light intensity is obtained in parallel for several spots on the sensor chip and analysed with a charged couple device (CCD) camera (Figure 3B). An SPRI sensor array allows to monitor many biological interactions at the same time and couples the sensitivity of scanning angle SPR measurements with the spatial capabilities of imaging in real-time [82]. Tokarzewicz et al. reported an SPRI sensor for MMP-1 that analysed light reflected from a sensor chip covered with a SAM functionalized with MMP-1 antibodies [79]. A linear response from 0.05 to 20 ng/mL was reported with an LOD of 9 pg/mL. This sensor was further

tested in plasma samples of healthy volunteers and patients with bladder cancer, providing results similar to ELISA tests. In a follow-up paper, Tokarzewicz et al. used the same design for an SPRI based MMP-2 sensor using an MMP-2 inhibitor (ARP 101) as recognition element [80]. The sensor had a linear response from 1 to 100 ng/mL with a LOD of 3.9 ng/mL and was used to determine MMP-2 levels in blood samples from healthy subjects and burned children.

Lyu and co-workers reported the development of an optical fibre-based system for the detection of MMP-3 and tumour necrosis factor alpha (TNF-α) in synovial fluid (Figure 3C) [78]. An uncladded region of an optical fibre was coated with gold nanoparticles functionalized with a SAM of mercaptoundecanoic acid (MUA) and mercapto-1-hexanol (MCH), and anti-MMP-3 or anti-TNF-α antibodies. In a diluted synovial fluid (1/25 in PBS buffer), the intensity decrease of the transmitted light due to antigen binding was the signal quantifying the enzyme down to the picomolar range.

While system resonance is classically induced by applying an external excitation at a suitable frequency, Fano resonance originates from the interference between two electromagnetic resonant modes of a multiresonant surface [83]. Nanopatterning of gold surfaces allows the coupling of a broadband wave (a continuum state) with the surface-bound state of the periodic nanostructured array (a discrete state), whose constructive and destructive interferences lead to an asymmetric Fano resonance (Figure 3D). The sharp slope of the Fano resonance peaks makes it suitable for measuring intensity shifts. In their gold nanoslit array, Wu et al. reported an intensity change in the Fano resonance of about 11,500% per refractive index unit (RIU) compared to 3,900% RIU of classical prism-based SPR, and such sensitivity could be increased to about 621,000% RIU using the integrated signal in the whole responsive range instead of a single wavelength. Human monocytic cells (THP1) were deposited on nanopatterned gold electrodes functionalized with anti-MMP-9 antibodies. After stimulating the cells by lipopolysaccharide (LPS) to produce the MMP-9, the intensity change at fixed wavelength was monitored in real time for 13 h [81].

Table 3. Analytical figures of merit relevant to SPR based sensors measuring MMPs. (SPR: Surface Plasmon Resonance, SPRI: Surface Plasmon Resonance Imaging, FOPPR: Fiber-optic particle plasmon resonance, RIU: Refractive Index Unit, A.U.: Arbitrary Units, LSPR: Localized Surface Plasmon Resonance).

Target	Reference	Year	Recognition	Signal transduction	Linear range	LOD	Sensitivity	Test solution	Additional Information
MMP-1	Tokarzewicz et al. [79]	2016	Antibody	SPRI	0.05-20 ng/mL	9pg/mL	$y(A.U.)=120 \cdot C_{MMP}+1974.7$	Human plasma	$R^2=0.997$ Sensor array: RSD = 1.6% (n = 24)
MMP-2	Pieper-Fürst et al. [75]	2004	TIMP Inhibitor	SPR	0.036 ng/mL-7.2 ng/mL (0.5-100 pM)[a]	0.036ng/mL (0.5pM)[a]	NA	PBS	NA Fabrication: RSD = 8.3% (n= 5)
	Tokarzewicz et al. [80]	2017	Inhibitor	SPRI	1-100 ng/mL	3.9 ng/mL	$y(A.U.)=36.321 \cdot C_{MMP}+1905.8$	Human Plasma	$R^2= 0.981$ Sensor array: RSD = 6.6% (n =36)
MMP-3	Huang et al. [78]	2013	Antibody	FOPPR	11 – 110 pg/mL(0.5-5 pM) [a]	34pg/mL	y(RIU)=5.18 10e7	Diluted synovial fluid	r =0.9996 Sensor: RSD = 1.25% (n=7)
MMP-9	Wu et al. [81]	2013	Antibody	SPR-grating	NA	NA	NA	Cell culture medium	Fabrication: RSD 2.6% (n=4)
	Mohseni et al. [76]	2016	Antibody	SPR	10-200 ng/mL	8pg /mL	y(RIU) = 3.01 10e6+ 179.43	Diluted saliva	$R^2=0.99$ Sensor: RSD < 8% (n = 9) Fabrication: RSD < 8% (n= 9)
MMP-14 (MT1-MMP)	Hong et al. [77]	2014	Peptide cleavage	LSPR	0.02- 2µg/mL	20ng/mL (1nM) [a]	NA	Cancer cell lysate	NA

3.2.3 Other optical sensor technologies

Other optical sensor technologies for MMP- detection exploit measurements of electroluminescence [84], photocurrent [85] and changes of fluorescence or the shift of peak positions of reflectance spectra in porous silicon surfaces [86–90] (Table 4).

Krismastuti et al. combined the capture of MMPs by antibody-modified magnetic nanoparticles with peptide cleavage in porous silicon resonant microcavities (pSiRM) [86]. Magnetic nanoparticles (magNP, 10 nm) were modified with anti-MMP-1 or anti-MMP-9 antibodies, incubated in diluted wound fluid or in solutions with known MMP-concentrations, and then released on a fluorogenic peptide-functionalized pSiRM. The active MMP, bound on the immuno-magNPs, cleaved the immobilized MMP peptide and the fluorescence from the fluorogenic dye was enhanced by the pSiRM.

Fan et al. fabricated an unusual photoelectrochemical biosensor for MMP-2 by coating a TiO_2 large bandgap (3.2eV) semiconductor electrode with lower bandgap sensitizers (CdS:Mn, 2.4 eV; CdTe, 1.7 eV) [84]. This multilayer structure was further modified with MMP-2-antibodies and incubated with PBS-buffer solutions containing MMP-2 concentrations in the range 10 fg/mL – 500 pg/mL. A sandwich structure formed after the addition of SiO_2 nanoparticles conjugated to a secondary MMP-2-antibody; the nanoparticles shaded the sensor surface and reduced the induced photocurrent.

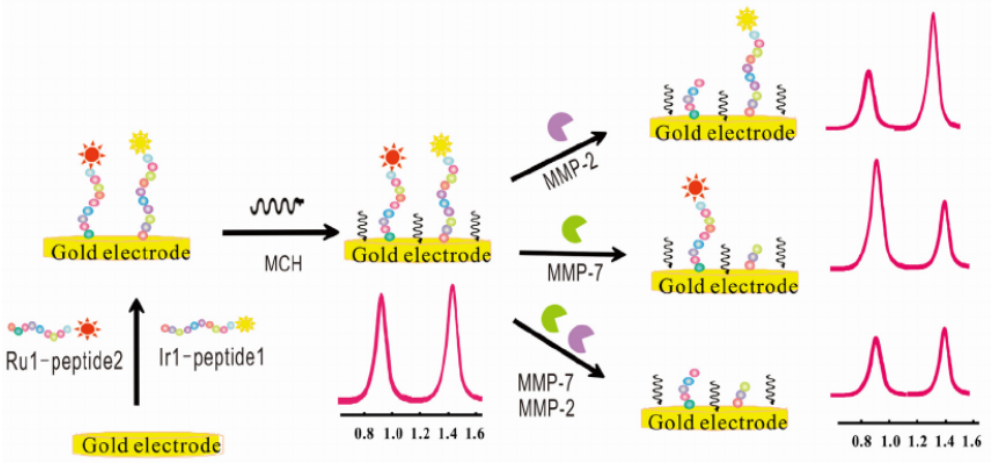

Figure 4. Schematic of electrochemical luminescence biosensor based on a luminescent peptide for the parallel detection of MMP-2 and MMP-7 [85]. (Reprinted from Sensors Actuators, B Chem., 253, Gao et al., Highly selective electrogenerated chemiluminescence biosensor for simultaneous detection of matrix metalloproteinase-2 and matrix metalloproteinase-7 in cell secretions, 69-76, Copyright (2017), with permission from Elsevier).

Gao et al. developed a multiplexed biosensor based on electrochemical luminescence (ECL) for the simultaneous detection of MMP-2 and MMP-7 in cell secretions [85]. In

ECL experiments, electrochemically produced species undergo electron transfer reactions and the products release light when relaxing the excited states [91]. In this work, iridium (III) and rutenium luminophore complexes were covalently labelled onto MMP-2- or MMP-7-specific peptide sequences and immobilized as self-assembled monolayers on gold electrodes (Figure 4).The application of positive potentials at +0.9 and +1.4 V vs Ag/AgCl in the presence of tripropylamine produced two well-separated strong ECL emissions. The hydrolysis of the specific peptide by the relevant MMP removed one of the metal complexes and decreased the intensity of the corresponding ECL emission. The calibration curves were linear in the ranges 10 ng/mL – 300 ng/mL (LOD 5 ng/mL) and 0.05 ng – 1 ng/mL (LOD 10 pg/mL) for MMP-2 and MMP-7, respectively. The biosensor was tested in living cells (HeLa, K562, HCT116 and macrophages) to detect the content of secreted MMP-2 and MMP-7.

In reflectance spectroscopy, a light beam is reflected from each layer of the incidence substrate. The reflected beams create an interference spectrum that changes according to the bioreactions at the surface of the substrate. [92] Porous silicon is an excellent substrate for reflectance spectroscopy since it can be functionalized with a high load of recognition sites, depending on the synthesis conditions, to achieve a high specific surface area (>200 m^2/cm^3) [93]. The positions of the reflectance peaks depend on the average refractive index of the surface [94]. Gooding and coworkers loaded the entire volume of pores of porous silicon with gelatine and monitored the shift in reflectance upon gelatine digestion by MMP-2 and 9. MMP-9 could be detected with 10 ng/mL LOD [89].

In a later publications, Gooding and coworkers optimized the sensor system using an ethylenglycol-based surface modification to reduce nonspecific binding [90] and reported the detection of MMP 2 and 9 of retinal pigment epithelial (RPE) cells and iris pigment epithelial (IPE) cells [88]. The cells were stimulated with different concentrations of lipopolysaccharide (LPS) (1, 2, 5 and 10 μg/mL) to secrete MMPs over 48 h. The amount of MMP-production was generally higher for MMP-2 than for MMP-9.

As an example of the use of antibodies for MMP detection on porous silicon surfaces, Martin et al. linked biotinylated bovine serum albumin to naked pSi and attached anti MMP-8 human antibody, previously modified with streptavidin, to sense MMP-8 [87]. After incubation, binding of MMP-8 in aqueous buffer solution was detected at a concentration of 100 ng/mL.

Table 4. Analytical figures of merit relevant to optical sensors measuring MMPs. (NA: not available)

Target	Reference	Publication year	Recognition	Signal transduction	Linear range	LOD	Sensitivity	Test solution	Additional Informatio
MMP-1	Kirsmastuti et al. [86]	2017	Peptide cleavage	Fluorescence	NA	NA	NA	Diluted human wound fluid	NA
MMP-2	Fan et al. [84]	2014	Antibody	Photocurrent	10fg/mL–500pg/mL	3.6fg/mL	I(μA) = 119.5 − 18.7 log(C_{MMP}) (pg/mL)	PBS	r = 0.997 Sensor: RSD = 2.1% (n = Fabrication: RSD = 3.5% (
	Gupta et al. [88]	2015	Peptide cleavage	Reflectometry	62 ng/mL – 6.2 μg/mL(1-100 nM)[a]	NA	NA	Cell culture medium	NA
	Gao et al. [85]	2017	Peptide cleavage	Electrochemical luminescence	10 ng/mL–300 ng/mL	5 ng/mL	ΔI(a.u.) = 3763·log(C_{MMP})+ 32105	Cell secretions	r = 0.996
	Kilian et al. [89]	2009	Peptide cleavage	Reflectometry	NA	NA	NA	Cell secretions	NA
	Soeriyadi et al.[90]	2014	Peptide cleavage	Reflectometry	6.2 μg/mL (100 nM)[a]	6.2 μg/mL (100 nM)[a]	NA	PBS	NA
MMP-7	Gao et al. [85]	2017	Peptide cleavage	Electrochemical luminescence	0.05 ng/mL–1ng/mL	10 pg/mL	ΔI(a.u) = 3812·log(C_{MMP})+ 41930	Cell secretions	r = 0.991
MMP-8	Martin et al. [87]	2011	Antibody	Reflectometry	NA	NA	NA	Phosphate buffer	NA
MMP-9	Gupta et al. [88]	2015	Peptide cleavage	Reflectometry	67 ng/mL – 6.7 μg/mL(1-100 nM)[a]	NA	NA	Cell culture	
	Krismastuti et al. [86]	2016	Peptide cleavage	Fluorescence	NA	NA	NA	Diluted human wound fluid	NA
	Kilian et al. [89]	2009	Peptide cleavage	Reflectometry	NA	10 ng/mL	NA	Cell secretion	NA
	Soeriyadi et al. [90]	2014	Peptide cleavage	Reflectometry	8.4 μg/mL (100 nM)[a]	8.4 μg/mL (100 nM)[a]	NA	PBS	NA

[a] Values converted from concentrations according to producer specifications

3.2.4 Other sensor technologies

In addition to electrochemical and optical sensors, literature reports other MMP biosensors such as field effect transistors (FETs) [95–100] and acoustic sensors like quartz-crystal microbalance (QCM) [101] and microcantilevers [102] (Table 5).

An FET is a transistor in which the charge carrier flow in the channel between the source and drain contacts is controlled by an electric field applied to the gate contact. Binding of molecules to the gate or to the dielectric between gate and channel changes the electric field and the intensity of the source-drain current. As usual, the critical issue is to coat the gate with materials, e.g. Si-nanowires [95,98,99], carbon nanotubes [96], SiO_2 [97] and reduced graphene oxide [100], selectively binding the target molecule. With the exception of Lee et al., who immobilized anti MMP-9 antibodies onto a carbon nanotube based gate [96], the general detection scheme exploits the MMP's proteolytic action of a specific protein. Choi et al. first proposed a Si-nanowire based FET for the detection of MMP-2 utilizing a specific peptide on the gate [98], then in a follow-up paper sensitivity was increased 12 to 14 fold by binding negatively charged DNA-Au nanoparticle complexes coupled with an MMP-2 specific peptide to the gate. The proteolytic action of MMP-2 released highly charged DNA fragments, leading to remarkable changes of surface charge and higher sensitivity.

In acoustic sensors, the mass variation resulting from the specific binding of a target analyte is quantified by measuring a frequency shift of a vibrating mechanical component. A quartz crystal microbalance (QCM) consists of a thin circular quartz slice whose shear motion is excited by a high frequency voltage applied to gold electrodes deposited on both faces. Soumetz et al. used ultra-thin precursor layers to immobilize a monolayer of monoclonal MMP-1 antibodies on a QCM electrode [101]. The QCM showed a nice linear response (sensitivity about 1.3 Hz/(ng/mL)) up to 150 ng/mL. Scarano et al. adopted a sandwich approach to recognize MMP-9 in human serum. A LOD of 560 pg/mL was obtained in diluted human serum by using the aptamers F3B, which was immobilized onto the QCM surface, and the biotinylated 8F14A [103]. In microcantilevers, the oscillating component is a microscopic silicon lever (about 100 nm) whose frequency shifts upon binding of the analyte. Specific peptide chains for membrane type-1 matrix metalloproteinase (MT1-MMP) were immobilized onto a microcantilever surface, and peptide hydrolysis allowed detection of MT1-MMP at concentrations 4.8 nM, 48 nM, and 480 nM [102].

Table 5. Analytical figures of merit of other sensors measuring MMPs (QCM: Quartz Crystal Microbalance, FET: Field-Effect-Transistor, NA: not available).

Target	Reference	Year	Recognition	Signal transduction	Linear range	LOD	Sensitivity	Test solution	Additional Information
MMP-1	Soumetz et al. [101]	2009	Antibody	QCM	35-150 ng/mL	NA	1.3 Hz/(ng/mL)	PBS	R^2=0.980
MMP-2	Yamamoto et al. [97]	2012	Peptide cleavage	FET	NA	NA	NA	PBS	NA
	Choi et al. [98]	2013	Peptide cleavage	FET	0.07ng/mL- 7.2µg/mL (1 pM-100 nM)[a]	NA	NA	PBS buffer	NA
	Choi et al. [99]	2013	Peptide cleavage	FET	0.007 ng/mL- 0.72µg/mL (0.1 pM-10 nM)[a]	0.007 ng/mL (0.1 pM)[a]	NA	PBS	NA
MMP-7	Chen et al [100]	2016	Peptide cleavage	FET	0.01-1 µg/mL	10 ng/mL	NA	Human plasma	NA
MMP-9	Lee et al. [95]	2009	Peptide cleavage	FET	NA	NA	NA	buffer (non specified)	NA
	Lee et al. [96]	2009	Antibody	FET	18-450 ng/mL	NA	NA	TRIS-buffer	NA
	Scarano et al. [103]	2015	Aptamers	QCM	0.1 – 2.5 nM	560 pg/mL	0.8 Hz/pM	Diluted human serum	NA
MT1-MMP-1	Lee et al. [102]	2012	Peptide cleavage	Microcantilever	96 ng/mL- 9.6 µg/mL (4.8-480 nM)[a]	NA	NA	Cell lysate	NA

[a]Values converted from concentrations according to producer specifications

4. Conclusions and future perspectives

In ageing societies, prevention and efficient management of golden age pathologies are fundamental for sustainable healthcare systems. Due to their ability to degrade extracellular matrix components and remodel tissues, MMPs have been associated with pathologies like cardiovascular diseases, inflammatory-based or degenerative pathologies and cancer, although their precise role still remains to be fully understood. Despite being regarded for a long time as the standard method to measure MMP activity, zymography can only be used for a subset of this large family of enzymes due to the limited choice of suitable substrates. This technique is simple, sensitive and allows separation of different forms of the same MMP but it can only provide semi-quantitative data. On the other hand, immunological methods such as ELISA permit quantitative analysis of a wider range of MMPs, but they cannot differentiate between active and inactive forms of the enzymes. Both techniques offer valuable information but are relatively expensive and require trained personnel in an analytical laboratory. Furthermore, a considerable variability of MMPs' basal levels is reported for healthy controls in different studies, thus suggesting a potential technique-related effect, in particular when different immunoassays are involved.

For these reasons, the perspective of new easy-to-use sensing technologies promising fast, reliable and cheap measurements is quite attractive. In this review, we grouped sensors measuring MMP concentrations or activities into four classes: electrochemical sensors, SPR based sensors, other optical sensors and sensors based on less common approaches (Table 6).

Electrochemical techniques are by far the preferred choice, whereas SPR and other optical sensors represent the second possible option. In fact, the number of studies devoted to optical sensing is comparable to that on electrochemical sensors, but these latter typically require a simpler and cheaper measurement electronics. Whatever the transduction technique, two basic approaches have been followed from most authors that recall differences between zymography and immunoassays. The first approach exploits the proteolytic action of MMPs: a "specific" peptide sequence is used to bind the transducer to the moiety generating or quenching the signal, so that once the sequence is cut the signal undergoes a substantial change. In this way, MMP activity is measured but the real selectivity of the peptide sequence is questionable. Binding of MMPs to antibodies, with several possible configurations, is the event generating the signal variation

according to the second approach. The advantage of immunochemical methods is high level of selectivity that can be achieved towards the target molecule, but at the same time antibodies are difficult to handle when fabricating the sensor (e.g. they have to be properly attached to the transducer to be able to bind the antigen), are expensive and need to be stored at low temperatures to avoid denaturation. In addition, no information is provided about the activity, as both active and inactive MMP forms are simultaneously detected. Comparing values reported in studies on MMP levels in nominally healthy subjects and patients with different pathologies, it is evident that sensors' limits of detection are more than suitable for measuring these enzymes in real samples. There are several examples in which these limits are two-three orders of magnitude lower than that required, but this gives the possibility to dilute the sample and reduce the matrix effect and the impact of chemical interferences. It is possible to argue that the chase for lower and lower limits of detection and innovative transduction methods is the effect of pressure exerted on the academic world towards publications. Proofing the reliability of research products seems much less fashionable, and many papers lacks evaluations of repeatability and reproducibility as well as reproducibility in sensor fabrication. In addition, only about half of the papers includes sensor tests in real samples. Sensor developers need to change this attitude for sensors to become ordinary analytical tools undergoing the same performance tests of analytical methods. Some biosensors use toxic materials, therefore the training of users to safety protocols and the waste disposal is another factor to be considered. To date, only companies have the potential of bridging the gap between research and clinical application, but, to the best of our knowledge, no commercial MMP sensor is yet available in a market largely dominated by ELISA kits. Developing a sensor requires substantial investments, and it is possible that the actual knowledge on the clinical value of MMP levels is still insufficient to guarantee a financial return in a reasonable time.

Table 6. Summary of methods used for the detection of MMPs

Method		Analyte	LOD	Pro	Cons	References
Zymography	Gelatine	MMP-2,9	0.12 ng	Mature; Sensitive; Separation of different analytes; Active and pro-enzymes detectable in parallel.	Limited substrate choice; Unable to differentiate active/inactive forms; Trained personnel necessary; Analytical laboratory necessary.	[17]
	Casein	MMP-3,7,10	0.013 ng			
ELISA		MMP-1,2,3,7,8, 20	0.01-10 ng	Mature; Sensitive; Quantitative.	Specific for one analyte only; No discrimination of active/inactive enzyme; Specialized personnel is necessary; Limited shelf-life of antibodies.	[17]
Molecular probes	Activity based probes	MMP-1,2,3,7,8,9,12,13	units of pg/mL	Labelling in vivo; Monitoring of target distributions.	No monitoring of dynamic processes; Often high synthetic effort.	[33,34,36,38,40–42,48,51,55]
	Substrate based probes	MMP-2,3,7,9,14	units of ng/mL			
	Antibody and other Affinity based probes	MMP-9, 14	-			
Electrochemical sensors	Voltammetric	MMP-2,3,7,9	5fg-5.6 ng/mL	Easy data acquisition; Low cost; Fast response; Portable devices readily available.	Possibly influenced by electronic interferences.	[57–61,63–66]
	Impedimetric	MMP-9	15-100 ng/mL			[68,69]
	Capacitive	MMP-9	0.93 ng/mL			[70]
Optical Sensors	SPR	MMP-1,2,3,9,14	8 pg-20 ng /mL	Not affected by electronic interferences; Often label-free Very Sensitive.	Aging of light source may interfere with measurement; Photobleaching of compounds.	[75–81]
	Fluorescence/Luminescence	MMP-1,2,7,9	10 pg-5 ng/mL			[85,86]
	Reflectometric	MMP-2,8,9	6.2-8.4 µg /mL			[87–90]
Other Sensors	FET	MMP-2,7,9	7 pg-10 ng/mL	Facile miniaturization and mass production.	Scarsely tested with real samples. Sensitivities mostly not reported	[95–100]
	QCM	MMP-1,9	0.56 ng/mL			[101,103]

Acknowledgments

Fondazione Pisa is gratefully acknowledged for partial support through the SEMPRE project.

References:

[1] S. Löffek, O. Schilling, C.-W. Franzke, Series “matrix metalloproteinases in lung health and disease”: Biological role of matrix metalloproteinases: a critical balance., Eur. Respir. J. (2011). doi:10.1183/09031936.00146510.

[2] D. Sbardella, G.F. Fasciglione, M. Gioia, C. Ciaccio, G.R. Tundo, S. Marini, M. Coletta, Human matrix metalloproteinases: An ubiquitarian class of enzymes involved in several pathological processes, Mol. Aspects Med. (2012). doi:10.1016/j.mam.2011.10.015.

[3] N. Funel, The role of miR-21 and miR-211 on MMP9 regulation in pancreatic ductal adenocarcinoma: Cooperation in invasiveness behaviors?, Epigenomics. (2015). doi:10.2217/epi.15.19.

[4] R. Roy, J. Yang, M.A. Moses, Matrix metalloproteinases as novel biomarkers and potential therapeutic targets in human cancer, J. Clin. Oncol. (2009). doi:10.1200/JCO.2009.23.5556.

[5] A. Jabłońska-Trypuć, M. Matejczyk, S. Rosochacki, Matrix metalloproteinases (MMPs), the main extracellular matrix (ECM) enzymes in collagen degradation, as a target for anticancer drugs, J. Enzyme Inhib. Med. Chem. (2016). doi:10.3109/14756366.2016.1161620.

[6] C. Tallant, A. Marrero, F.X. Gomis-Rüth, Matrix metalloproteinases: Fold and function of their catalytic domains, Biochim. Biophys. Acta - Mol. Cell Res. (2010). doi:10.1016/j.bbamcr.2009.04.003.

[7] H. Nagase, R. Visse, G. Murphy, Structure and function of matrix metalloproteinases and TIMPs, Cardiovasc. Res. (2006). doi:10.1016/j.cardiores.2005.12.002.

[8] G. Murphy, H. Nagase, Progress in matrix metalloproteinase research, Mol. Aspects Med. (2009). doi:10.1016/j.mam.2008.05.002.

[9] A. Doucet, G.S. Butler, D. Rodríguez, A. Prudova, C.M. Overall, Metadegradomics: toward in vivo quantitative degradomics of proteolytic post-translational modifications of the cancer proteome., Mol. Cell. Proteomics. (2008). doi:10.1074/mcp.R800012-MCP200.

[10] C.J. Morrison, G.S. Butler, D. Rodríguez, C.M. Overall, Matrix metalloproteinase proteomics: substrates, targets, and therapy, Curr. Opin. Cell Biol. (2009). doi:10.1016/j.ceb.2009.06.006.

[11] T. Klein, R. Bischoff, Physiology and pathophysiology of matrix metalloproteases, Amino Acids. (2011). doi:10.1007/s00726-010-0689-x.

[12] K.L. Andarawewa, A. Boulay, R. Masson, C. Mathelin, I. Stoll, C. Tomasetto, M.P. Chenard, M. Gintz, J.P. Bellocq, M.C. Rio, Dual stromelysin-3 function during natural mouse mammary tumor virus-ras tumor progression, Cancer Res. (2003). doi:10.1038/356397a0.

[13] V.R. Krishnaswamy, D. Mintz, I. Sagi, Matrix metalloproteinases: The sculptors of chronic cutaneous wounds, Biochim. Biophys. Acta - Mol. Cell Res. (2017). doi:10.1016/j.bbamcr.2017.08.003.

[14] A. Alaseem, K. Alhazzani, P. Dondapati, S. Alobid, A. Bishayee, A. Rathinavelu, Matrix Metalloproteinases: A challenging paradigm of cancer management, Semin. Cancer Biol. (2017). doi:10.1016/j.semcancer.2017.11.008.

[15] C. López-Otín, L.M. Matrisian, Emerging roles of proteases in tumour suppression, Nat. Rev. Cancer. (2007). doi:10.1038/nrc2228.

[16] C. Lombard, J. Saulnier, J. Wallach, Assays of matrix metalloproteinases (MMPs) activities: A review, Biochimie. (2005). doi:10.1016/j.biochi.2005.01.007.

[17] S. Krizkova, O. Zitka, V. Adam, R. Kizek, M. Masarik, M. Stiborova, T. Eckschlager, G.J. Chavis, Assays for determination of matrix metalloproteinases and their activity, TrAC - Trends Anal. Chem. (2011). doi:10.1016/j.trac.2011.06.016.

[18] I.M. Clark, Matrix Metalloproteinase Protocols, Humana Press, 2001.

[19] S. Chakraborti, M. Mandal, S. Das, A. Mandal, T. Chakraborti, Regulation of matrix metalloproteinases. An overview, Mol. Cell. Biochem. (2003). doi:10.1023/A:1026028303196.

[20] M. Koulentaki, V. Valatas, K. Xidakis, A. Kouroumalis, E. Petinaki, E. Castanas, E. Kouroumalis, Matrix metalloproteinases and their inhibitors in acute viral hepatitis, J. Viral Hepat. (2002). doi:10.1046/j.1365-2893.2002.00351.x.

[21] B. Schwartzkopff, M. Fassbach, B. Pelzer, M. Brehm, B.E. Strauer, Elevated serum markers of collagen degradation in patients with mild to moderate dilated cardiomyopathy, Eur. J. Heart Fail. (2002). doi:10.1016/s1388-9842(02)00092-2.

[22] K. Masuhara, T. Nakai, K. Yamaguchi, S. Yamasaki, Y. Sasaguri, Significant increases in serum and plasma concentrations of matrix metalloproteinases 3 and 9 in patients with rapidly destructive osteoarthritis of the hip, Arthritis Rheum. (2002). doi:10.1002/art.10547.

[23] M. Roderfeld, T. Rath, R. Schulz, W. Seeger, A. Tschuschner, J. Graf, E. Roeb, Serum matrix metalloproteinases in adult CF patients: Relation to pulmonary exacerbation, J. Cyst. Fibros. (2009). doi:10.1016/j.jcf.2009.06.001.

[24] M. Groblewska, B. Mroczko, M. Gryko, A. Pryczynicz, K. Guzińska-Ustymowicz, B. K□dra, A. Kemona, M. Szmitkowski, Serum levels and tissue expression of matrix metalloproteinase 2 (MMP-2) and tissue inhibitor of metalloproteinases 2 (TIMP-2) in colorectal cancer patients, Tumor Biol. (2014). doi:10.1007/s13277-013-1502-8.

[25] A.M.J. Langers, H.W. Verspaget, L.J.A.C. Hawinkels, F.J.G.M. Kubben, W. Van Duijn, J.J. Van Der Reijden, J.C.H. Hardwick, D.W. Hommes, C.F.M. Sier, MMP-2 and MMP-9 in normal mucosa are independently associated with outcome of colorectal cancer patients, Br. J. Cancer. (2012). doi:10.1038/bjc.2012.80.

[26] H. Yamanaka, Y. Matsuda, M. Tanaka, W. Sendo, H. Nakajima, A. Taniguchi, N. Kamatani, Serum matrix metalloproteinase 3 as a predictor of the degree of joint destruction during the six months after measurement, in patients with early rheumatoid arthritis, Arthritis Rheum. (2000). doi:10.1002/1529-0131(200004)43:4<852::AID-ANR16>3.0.CO;2-7.

[27] J. Guiot, M. Henket, J.L. Corhay, C. Moermans, R. Louis, Sputum biomarkers in IPF: Evidence for raised gene expression and protein level of IGFBP-2, IL-8 and MMP-7, PLoS One. (2017). doi:10.1371/journal.pone.0171344.

[28] J.P. Väyrynen, J. Vornanen, T. Tervahartiala, T. Sorsa, R. Bloigu, T. Salo, A. Tuomisto, M.J. Mäkinen, Serum MMP-8 levels increase in colorectal cancer and correlate with disease course and inflammatory properties of primary tumors, Int. J. Cancer. (2012). doi:10.1002/ijc.26435.

[29] V.D. Nadarajah, M. van Putten, A. Chaouch, P. Garrood, V. Straub, H. Lochmüller, H.B. Ginjaar, A.M. Aartsma-Rus, G.J.B. van Ommen, J.T. den Dunnen, P.A.C. ’t Hoen, Serum matrix metalloproteinase-9 (MMP-9) as a biomarker for monitoring disease progression in Duchenne muscular dystrophy (DMD), Neuromuscul. Disord. (2011). doi:10.1016/j.nmd.2011.05.011.

[30] P. Laudański, J. Światecka, L. Kozłwski, M. Leśniewska, M. Wojtukiewicz, S. Wolczyński, Increased serum level of membrane type 1-matrix metalloproteinase (MT1-MMP/MMP-14) in patients with breast cancer, Folia Histochem. Cytobiol. (2010). doi:10.2478/v10042-009-0085-0.

[31] J. Vandooren, P.E. Van Den Steen, G. Opdenakker, Biochemistry and molecular biology of gelatinase B or matrix metalloproteinase-9 (MMP-9): The next decade, Crit. Rev. Biochem. Mol. Biol. (2013). doi:10.3109/10409238.2013.770819.
[32] D. Thevenot, K. Toth, R. Durst, G. Wilson, D. Thevenot, K. Toth, R. Durst, G. Wilson, K. Toth, R.A. Durst, G.S. Wilson, Electrochemical biosensors□: recommended definitions and classification To cite this version□: HAL Id□: hal-01084678 Technical report Electrochemical biosensors□: recommended definitions and classification, Biosens. Bioelectron. (2001).
[33] M. Fonović, M. Bogyo, Activity-based probes as a tool for functional proteomic analysis of proteases, Expert Rev. Proteomics. (2008). doi:10.1586/14789450.5.5.721.
[34] S.A. Sieber, S. Niessen, H.S. Hoover, B.F. Cravatt, Proteomic profiling of metalloprotease activities with cocktails of active-site probes, Nat. Chem. Biol. (2006). doi:10.1038/nchembio781.
[35] A. Saghatelian, N. Jessani, A. Joseph, M. Humphrey, B.F. Cravatt, Activity-based probes for the proteomic profiling of metalloproteases, Proc. Natl. Acad. Sci. (2004). doi:10.1073/pnas.0402784101.
[36] C. Nury, B. Czarny, E. Cassar-Lajeunesse, D. Georgiadis, S. Bregant, V. Dive, A Pan Photoaffinity Probe for Detecting Active Forms of Matrix Metalloproteinases, ChemBioChem. (2013). doi:10.1002/cbic.201200583.
[37] H.Y. Hu, S. Gehrig, G. Reither, D. Subramanian, M.A. Mall, O. Plettenburg, C. Schultz, FRET-based and other fluorescent proteinase probes, Biotechnol. J. (2014). doi:10.1002/biot.201300201.
[38] R. Fudala, R. Rich, A. Mukerjee, A. Ranjan, J. Vishwanatha, A. Kurdowska, Z. Gryczynski, J. Borejdo, I. Gryczynski, Fluorescence Detection of MMP-9. II. Ratiometric FRET-Based Sensing With Dually Labeled Specific Peptide, Curr. Pharm. Biotechnol. (2014). doi:10.2174/1389201014131406051111109.
[39] T.J. Lively, D.B. Bosco, Z.I. Khamis, Q.X. Amy Sang, Assessment of synthetic matrix metalloproteinase inhibitors by fluorogenic substrate assay, in: Methods Mol. Biol., 2016. doi:10.1007/978-1-4939-3444-7_13.
[40] Z. Lei, H. Chen, H. Zhang, Y. Wang, X. Meng, Z. Wang, Evaluation of Matrix Metalloproteinase Inhibition by Peptide Microarray-Based Fluorescence Assay on Polymer Brush Substrate and in Vivo Assessment, ACS Appl. Mater. Interfaces. (2017). doi:10.1021/acsami.7b15445.
[41] P.J. Kraft, D.E. Haynes-Johnson, L. Patel, J.A. Lenhart, R.A. Zivin, S.S. Palmer, Fluorescence polarization assay and SDS-PAGE confirms matrilysin degrades fibronectin and collagen IV whereas gelatinase a degrades collagen IV but not fibronectin, Connect. Tissue Res. (2001). doi:10.3109/03008200109014256.
[42] A. Knapinska, G.B. Fields, Chemical Biology for Understanding Matrix Metalloproteinase Function, ChemBioChem. (2012). doi:10.1002/cbic.201200298.
[43] W.J. Akers, B. Xu, H. Lee, G.P. Sudlow, G.B. Fields, S. Achilefu, W.B. Edwards, Detection of MMP-2 and MMP-9 activity in vivo with a triple-helical peptide optical probe, Bioconjug. Chem. (2012). doi:10.1021/bc300027y.
[44] G.B. Kim, Y.-P. Kim, Analysis of Protease Activity Using Quantum Dots and Resonance Energy Transfer, Theranostics. (2012). doi:10.7150/thno.3476.
[45] L. Shi, V. De Paoli, N. Rosenzweig, Z. Rosenzweig, Synthesis and application of quantum dots FRET-based protease sensors, J. Am. Chem. Soc. (2006). doi:10.1021/ja063509o.
[46] H. Lee, Y.P. Kim, Fluorescent and bioluminescent nanoprobes for in vitro and in vivo detection of matrix metalloproteinase activity, BMB Rep. (2015). doi:10.5483/BMBRep.2015.48.6.054.
[47] E. Song, D. Cheng, Y. Song, M. Jiang, J. Yu, Y. Wang, A graphene oxide-based FRET sensor for rapid and sensitive detection of matrix metalloproteinase 2 in human serum sample, Biosens. Bioelectron. (2013). doi:10.1016/j.bios.2013.03.030.
[48] Y.P. Kim, W.L. Daniel, Z. Xia, H. Xie, C.A. Mirkin, J. Rao, Bioluminescent nanosensors for protease detection based upon gold nanoparticle-luciferase conjugates, Chem. Commun. (2010). doi:10.1039/b915612g.
[49] H. Yao, Y. Zhang, F. Xiao, Z. Xia, J. Rao, Quantum dot/bioluminescence resonance energy transfer based highly sensitive detection of proteases, Angew. Chemie - Int. Ed. (2007). doi:10.1002/anie.200700280.
[50] Z. Xia, Y. Xing, J. Jeon, Y.P. Kim, J. Gall, A. Dragulescu-Andrasi, S.S. Gambhir, J. Rao, Immobilizing reporters for molecular imaging of the extracellular microenvironment in living animals, ACS Chem. Biol. (2011). doi:10.1021/cb200135e.
[51] Y. Park, Y.M. Ryu, Y. Jung, T. Wang, Y. Baek, Y. Yoon, S.M. Bae, J. Park, S. Hwang, J. Kim, E.J. Do, S.Y. Kim, E. Chung, K.H. Kim, S. Kim, S.J. Myung, Spraying quantum dot conjugates in the colon of live animals enabled rapid and multiplex cancer diagnosis using endoscopy, ACS Nano. (2014). doi:10.1021/nn5009269.
[52] Z. Wang, G. Deng, Z. Zhang, H. Huang, Y. Zhao, Noninvasive detection of matrix metalloproteinase-9 in atherosclerotic lesions using technetium-99m-labeled single-photon emission computed tomography in vivo, (2017). doi:10.1097/MNM.0000000000000651.
[53] S. Song, L. Wang, J. Li, C. Fan, J. Zhao, Aptamer-based biosensors, TrAC - Trends Anal. Chem. (2008). doi:10.1016/j.trac.2007.12.004.
[54] S. Da Rocha Gomes, J. Miguel, L. Azéma, S. Eimer, C. Ries, E. Dausse, H. Loiseau, M. Allard, J.J. Toulmé, 99mTc-MAG3-aptamer for imaging human tumors associated with high level of matrix metalloprotease-9, Bioconjug. Chem. (2012). doi:10.1021/bc300146c.
[55] D. Kryza, F. Debordeaux, L. Azéma, A. Hassan, O. Paurelle, J. Schulz, C. Savona-Baron, E. Charignon, P. Bonazza, J. Taleb, P. Fernandez, M. Janier, J.J. Toulmé, Ex vivo and in vivo imaging and biodistribution of aptamers targeting the human Matrix MetalloProtease-9 in melanomas, PLoS One. (2016). doi:10.1371/journal.pone.0149387.
[56] C.M.A. Brett, A.M.O. Brett, Step and pulse techniques, Encycl. Electrochem. Vol. 3 Instrum. Electroanal. Chem. (2007) 199–222. doi:10.1002/9783527610426.bard030202.
[57] W. Xu, P. Jing, H. Yi, S. Xue, R. Yuan, Bimetallic Pt/Pd encapsulated mesoporous-hollow CeO2nanospheres for signal amplification toward electrochemical peptide-based biosensing for matrix metalloproteinase 2, Sensors Actuators, B Chem. 230 (2016) 345–352. doi:10.1016/j.snb.2016.02.064.
[58] D. Wang, Y. Yuan, Y. Zheng, Y. Chai, R. Yuan, An electrochemical peptide cleavage-based biosensor for matrix metalloproteinase-2 detection with exonuclease III-assisted cycling signal amplification, Chem. Commun. (2016). doi:10.1039/c6cc00928j.
[59] G. Liu, J. Wang, D.S. Wunschel, Y. Lin, Electrochemical proteolytic beacon for detection of matrix metalloproteinase activities, J. Am. Chem. Soc. (2006). doi:10.1021/ja0626638.
[60] H. Xu, H. Ye, L. Yu, Y. Chi, X. Liu, G. Chen, Tailor-made peptide sensor for detection of matrix metalloproteinase 2 in blood serum, Anal. Methods. 7 (2015) 5371–5374. doi:10.1039/c5ay00666j.
[61] P. Jing, H. Yi, S. Xue, R. Yuan, W. Xu, A “signal on-off” electrochemical peptide biosensor for matrix metalloproteinase 2 based on target induced cleavage of a peptide, RSC Adv. 5 (2015) 65725–65730. doi:10.1039/c5ra10662a.
[62] J.W. Lee, J.Y. Yun, W.C. Lee, S. Choi, J.H. Lim, H. Jeong, D.S. Shin, Y.J. Park, A reference electrode-free

electrochemical biosensor for detecting MMP-9 using a concentric electrode device, Sensors Actuators, B Chem. 240 (2017) 735–741. doi:10.1016/j.snb.2016.09.026.
[63] D.S. Shin, Y. Liu, Y. Gao, T. Kwa, Z. Matharu, A. Revzin, Micropatterned surfaces functionalized with electroactive peptides for detecting protease release from cells, Anal. Chem. (2013). doi:10.1021/ac302547p.
[64] G. Yang, L. Li, R.K. Rana, J.J. Zhu, Assembled gold nanoparticles on nitrogen-doped graphene for ultrasensitive electrochemical detection of matrix metalloproteinase-2, Carbon N. Y. 61 (2013) 357–366. doi:10.1016/j.carbon.2013.05.016.
[65] J.J. Shi, T.T. He, F. Jiang, E.S. Abdel-Halim, J.J. Zhu, Ultrasensitive multi-analyte electrochemical immunoassay based on GNR-modified heated screen-printed carbon electrodes and PS@PDA-metal labels for rapid detection of MMP-9 and IL-6, Biosens. Bioelectron. 55 (2014) 51–56. doi:10.1016/j.bios.2013.11.056.
[66] B.S. Munge, J. Fisher, L.N. Millord, C.E. Krause, R.S. Dowd, J.F. Rusling, Sensitive electrochemical immunosensor for matrix metalloproteinase-3 based on single-wall carbon nanotubes, Analyst. 135 (2010) 1345–1350. doi:10.1039/c0an00028k.
[67] B.-Y. Chang, S.-M. Park, Electrochemical Impedance Spectroscopy, Annu. Rev. Anal. Chem. 3 (2010) 207–229. doi:10.1146/annurev.anchem.012809.102211.
[68] I. Ciani, H. Schulze, D.K. Corrigan, G. Henihan, G. Giraud, J.G. Terry, A.J. Walton, R. Pethig, P. Ghazal, J. Crain, C.J. Campbell, T.T. Bachmann, A.R. Mount, Development of immunosensors for direct detection of three wound infection biomarkers at point of care using electrochemical impedance spectroscopy, Biosens. Bioelectron. 31 (2012) 413–418. doi:10.1016/j.bios.2011.11.004.
[69] A. Biela, M. Watkinson, U.C. Meier, D. Baker, G. Giovannoni, C.R. Becer, S. Krause, Disposable MMP-9 sensor based on the degradation of peptide cross-linked hydrogel films using electrochemical impedance spectroscopy, Biosens. Bioelectron. 68 (2015) 660–667. doi:10.1016/j.bios.2015.01.060.
[70] T.B. Tran, P.D. Nguyen, C. Baek, J. Min, Electrical dual-sensing method for real-time quantitative monitoring of cell-secreted MMP-9 and cellular morphology during migration process, Biosens. Bioelectron. 77 (2016) 631–637. doi:10.1016/j.bios.2015.10.030.
[71] L. Wang, H. Wang, L. Wang, K. Mitchelson, Z. Yu, J. Cheng, Analysis of the sensitivity and frequency characteristics of coplanar electrical cell-substrate impedance sensors, Biosens. Bioelectron. (2008). doi:10.1016/j.bios.2008.03.018.
[72] J. Homola, Surface plasmon resonance sensors for detection of chemical and biological species., Chem. Rev. (2008). doi:10.1021/cr068107d.
[73] J. Homola, S.S. Yee, G. Gauglitz, Surface plasmon resonance sensors: review, Sensors Actuators B Chem. (1999). doi:10.1016/S0925-4005(98)00321-9.
[74] P. Salvo, V. Dini, A. Kirchhain, A. Janowska, T. Oranges, A. Chiricozzi, T. Lomonaco, F. Di Francesco, M. Romanelli, Sensors and biosensors for C-reactive protein, temperature and pH, and their applications for monitoring wound healing: A review, Sensors (Switzerland). (2017). doi:10.3390/s17122952.
[75] U. Pieper-Fürst, U. Kleuser, W.F.M. Stöcklein, A. Warsinke, F.W. Scheller, Detection of subpicomolar concentrations of human matrix metalloproteinase-2 by an optical biosensor, Anal. Biochem. 332 (2004) 160–167. doi:10.1016/j.ab.2004.05.047.
[76] S. Mohseni, T.T. Moghadam, B. Dabirmanesh, S. Jabbari, K. Khajeh, Development of a label-free SPR sensor for detection of matrixmetalloproteinase-9 by antibody immobilization on carboxymethyldextran chip, Biosens. Bioelectron. 81 (2016) 510–516. doi:10.1016/j.bios.2016.03.038.
[77] Y. Hong, M. Ku, E. Lee, J.-S. Suh, Y.-M. Huh, D.S. Yoon, J. Yang, Localized surface plasmon resonance based nanobiosensor for biomarker detection of invasive cancer cells, J. Biomed. Opt. 19 (2013) 051202. doi:10.1117/1.JBO.19.5.051202.
[78] Y.C. Huang, C.Y. Chiang, C.H. Li, T.C. Chang, C.S. Chiang, L.K. Chau, K.W. Huang, C.W. Wu, S.C. Wang, S.R. Lyu, Quantification of tumor necrosis factor-α and matrix metalloproteinases-3 in synovial fluid by a fiber-optic particle plasmon resonance sensor, Analyst. 138 (2013) 4599–4606. doi:10.1039/c3an00276d.
[79] A. Tokarzewicz, L. Romanowicz, I. Sveklo, E. Gorodkiewicz, R. Li, X. Qin, S. Li, A. Roessner, The development of a matrix metalloproteinase-1 biosensor based on the surface plasmon resonance imaging technique, Anal. Methods. 8 (2016) 6428–6435. doi:10.1039/C6AY01856D.
[80] A. Tokarzewicz, L. Romanowicz, I. Sveklo, E. Matuszczak, A. Hermanowicz, E. Gorodkiewicz, SPRI biosensors for quantitative determination of matrix metalloproteinase-2, Anal. Methods. 9 (2017) 2407–2414. doi:10.1039/c7ay00786h.
[81] S.H. Wu, K.L. Lee, A. Chiou, X. Cheng, P.K. Wei, Optofluidic platform for real-time monitoring of live cell secretory activities using Fano resonance in gold nanoslits, Small. 9 (2013) 3532–3540. doi:10.1002/smll.201203125.
[82] S. Scarano, M. Mascini, A.P.F. Turner, M. Minunni, Surface plasmon resonance imaging for affinity-based biosensors, Biosens. Bioelectron. (2010). doi:10.1016/j.bios.2009.08.039.
[83] A.E. Miroshnichenko, S. Flach, Y.S. Kivshar, Fano resonances in nanoscale structures, Rev. Mod. Phys. 82 (2010) 2257–2298. doi:10.1103/RevModPhys.82.2257.
[84] G.C. Fan, L. Han, H. Zhu, J.R. Zhang, J.J. Zhu, Ultrasensitive photoelectrochemical immunoassay for matrix metalloproteinase-2 detection based on CdS:Mn/CdTe cosensitized TiO2nanotubes and signal amplification of SiO2@Ab2conjugates, Anal. Chem. 86 (2014) 12398–12405. doi:10.1021/ac504027d.
[85] H. Gao, Q. Dang, S. Xia, Y. Zhao, H. Qi, Q. Gao, C. Zhang, Highly selective electrogenerated chemiluminescence biosensor for simultaneous detection of matrix metalloproteinase-2 and matrix metalloproteinase-7 in cell secretions, Sensors Actuators, B Chem. 253 (2017) 69–76. doi:10.1016/j.snb.2017.05.142.
[86] F.S.H. Krismastuti, M.R. Dewi, B. Prieto-Simon, T. Nann, N.H. Voelcker, Disperse-and-Collect Approach for the Type-Selective Detection of Matrix Metalloproteinases in Porous Silicon Resonant Microcavities, ACS Sensors. 2 (2017) 203–209. doi:10.1021/acssensors.6b00442.
[87] M. Martin, C. Taleb Bendiab, L. Massif, G. Palestino, V. Agarwal, F. Cuisinier, C. Gergely, Matrix metalloproteinase sensing via porous silicon microcavity devices functionalized with human antibodies, Phys. Status Solidi Curr. Top. Solid State Phys. 8 (2011) 1888–1892. doi:10.1002/pssc.201000155.
[88] B. Gupta, K. Mai, S.B. Lowe, D. Wakefield, N. Di Girolamo, K. Gaus, P.J. Reece, J.J. Gooding, Ultrasensitive and Specific Measurement of Protease Activity Using Functionalized Photonic Crystals, Anal. Chem. 87 (2015) 9946–9953. doi:10.1021/acs.analchem.5b02529.
[89] K.A. Kilian, L.M.H. Lai, A. Magenau, S. Cartland, T. Bocking, N. Di Girolamo, M. Gal, K. Gaus, J.J. Gooding, Smart tissue culture: in situ monitoring of the activity of protease enzymes secreted from live cells using nanostructured photonic crystals, Nano Lett. 9 (2009) 2021–2025. doi:10.1021/nl900283j.
[90] A.H. Soeriyadi, B. Gupta, P.J. Reece, J.J. Gooding, Optimising the enzyme response of a porous silicon photonic crystal

via the modular design of enzyme sensitive polymers, Polym. Chem. (2014). doi:10.1039/c3py01638b.
[91] P. Bertoncello, R.J. Forster, Nanostructured materials for electrochemiluminescence (ECL)-based detection methods: Recent advances and future perspectives, Biosens. Bioelectron. (2009). doi:10.1016/j.bios.2009.02.013.
[92] M.B. Wallace, A. Wax, D.N. Roberts, R.N. Graf, Reflectance Spectroscopy, Gastrointest. Endosc. Clin. N. Am. (2009).
[93] G. Bomchil, R. Herino, K. Barla, J.C. Pfister, Pore Size Distribution in Porous Silicon Studied by Adsorption Isotherms, J. Electrochem. Soc. (1983). doi:10.1149/1.2120044.
[94] L. Canham, Handbook of Porous Silicon, 2014. doi:10.1007/978-3-319-05744-6.
[95] S.H. Lee, K.J. Jeon, W. Lee, A. Choi, H. Il Jung, C.J. Kim, M.H. Jo, P-type Si-nanowire-based field-effect transistors for electric detection of a biomarker: Matrix metalloproteinase-9, J. Korean Phys. Soc. 55 (2009) 232–235. doi:10.3938/jkps.55.232.
[96] H.S. Lee, J.S. Oh, Y.W. Chang, Y.J. Park, J.S. Shin, K.H. Yoo, Carbon nanotube-based biosensor for detection of matrix metallopeptidase-9 and S-100B, Curr. Appl. Phys. 9 (2009) e270–e272. doi:10.1016/j.cap.2009.07.003.
[97] D. Yamamoto, S. Hideshima, S. Kuroiwa, T. Nakanishi, T. Osaka, Detection of matrix metalloproteinase-2 by field effect transistor with a fibronectin-immobilized gate, Chem. Lett. (2012). doi:10.1246/cl.2012.825.
[98] J.H. Choi, H. Kim, H.S. Kim, S.H. Um, J.W. Choi, B.K. Oh, MMP-2 detective silicon nanowire biosensor using enzymatic cleavage reaction, J. Biomed. Nanotechnol. 9 (2013) 732–735. doi:10.1166/jbn.2013.1541.
[99] J.H. Choi, H. Kim, J.H. Choi, J.W. Choi, B.K. Oh, Signal enhancement of silicon nanowire-based biosensor for detection of matrix metalloproteinase-2 using DNA-Au nanoparticle complexes, ACS Appl. Mater. Interfaces. 5 (2013) 12023–12028. doi:10.1021/am403816x.
[100] H. Chen, P. Chen, J. Huang, R. Selegård, M. Platt, A. Palaniappan, D. Aili, A.I.Y. Tok, B. Liedberg, Detection of Matrilysin Activity Using Polypeptide Functionalized Reduced Graphene Oxide Field-Effect Transistor Sensor, Anal. Chem. 88 (2016) 2994–2998. doi:10.1021/acs.analchem.5b04663.
[101] F.C. Soumetz, L. Pastorino, C. Ruggiero, Development of a piezoelectric immunosensor for matrix metalloproteinase-1 detection, in: Proc. 31st Annu. Int. Conf. IEEE Eng. Med. Biol. Soc. Eng. Futur. Biomed. EMBC 2009, 2009. doi:10.1109/IEMBS.2009.5333860.
[102] G. Lee, K. Eom, J. Park, J. Yang, S. Haam, Y.M. Huh, J.K. Ryu, N.H. Kim, J.I. Yook, S.W. Lee, D.S. Yoon, T. Kwon, Real-time quantitative monitoring of specific peptide cleavage by a proteinase for cancer diagnosis, Angew. Chemie - Int. Ed. 51 (2012) 5837–5841. doi:10.1002/anie.201108830.
[103] S. Scarano, E. Dausse, F. Crispo, J.J. Toulmé, M. Minunni, Design of a dual aptamer-based recognition strategy for human matrix metalloproteinase 9 protein by piezoelectric biosensors, Anal. Chim. Acta. (2015). doi:10.1016/j.aca.2015.07.009.

CAPTIONS

Figure 1. Multi-domain structure of human metalloproteinases (MMPs). S, signal peptide (signal anchor in MMP-23); Pro, pro-peptide; Cat, catalytic domain; Zn, Zn containing active site; H, hinge region; Fn, fibronectin insert; F, furin cleavage site; I, type I transmembrane domain; Cp, cytoplasmic domain; G, glycosylphosphatidyl inositol (GPI) anchoring domain; II, type II transmembrane domain; Ca, cysteine-rich domain; Ig, Immunoglobulin-like domain.

Figure 2. General principle of turn-on and turn off strategy. A) Turn on-probes: the proteolytic interaction produces free sites for the attachment of the redox mediator and the signal intensity increases. B) Turn-off probes: redox mediators are removed from the sensor surface by the enzymatic activity and the signal intensity decreases.

Figure 3. SPR based techniques in biosensors:

(A): Sensor chip using Kretschmann geometry covered with carboxymethyldextran (CMD) conjugated with anti-MMP-9 antibodies to measure MMP-9 concentration in diluted saliva samples [76]. (Reprinted from Biosens. Bioelectron. 81, Mohseni et al., Development of a label-free SPR sensor for detection of matrixmetalloproteinase-9 by antibody immobilization on carboxymethyldextran chip, 510-516, 2016, with permission from Elsevier.)

(B) SPR imaging chip for the parallel detection in real time of different functionalities [82]. (Reprinted from Biosens. Bioelectron., 25(5), Scarano et al., Surface plasmon resonance imaging for affinity-based biosensors, 957-966, 2010, with permission from Elsevier.)

(C) Binding of antigens to antibodies of a functionalized optic fibre resulting in enhanced absorbance of the sensing layer and reduced transmission of light [78].

(D) Experimental setup for the label-free detection of cell secretion according to [81] (Reprinted from Small, 9, Wu et al, Optofluidic platform for real-time monitoring of live cell secretory activities using Fano resonance in gold nanoslits, 3532-3540,2013, with permission from John Wiley and Sons) and depiction of the Fano resonance as a superposition of discrete and continuous resonance modes of nanopatterned surfaces [83]. (Reprinted figure with permission from Miroshnichenko et al., Rev. Mod. Phys., 82, 2257-2298, 2010. Copyright (2010) American Physical Society).

Figure 4. Schematic of electrochemical luminescence biosensor based on a luminescent peptide for the parallel detection of MMP-2 and MMP-7 [85]. (Reprinted from Sensors Actuators, B Chem., 253, Gao et al., Highly selective electrogenerated chemiluminescence biosensor for simultaneous detection of matrix metalloproteinase-2 and matrix metalloproteinase-7 in cell secretions, 69-76, Copyright (2017), with permission from Elsevier).

Table 1. Functional properties and concentrations of selected human matrix metalloproteinases in healthy subjects and in patients with different diseases.

Table 2. Analytical figures of merit relevant to electrochemical sensors measuring MMPs. (DPV: Differential Pulse Voltammetry, SWV: Square Wave Voltammetry, CV: Cyclic Voltammetry, NA: not available).

Table 3. Analytical figures of merit relevant to SPR based sensors measuring MMPs. (SPR: Surface Plasmon Resonance, SPRI: Surface Plasmon Resonance Imaging, FOPPR: Fiber-Optic Particle Plasmon resonance, RIU: Refractive Index Unit, A.U.: Arbitrary Units, LSPR: Localized Surface Plasmon Resonance).

Table 4. Analytical figures of merit relevant to optical sensors measuring MMPs. (NA: not available)

Table 5. Analytical figures of merit of other sensors measuring MMPs (QCM: Quartz Crystal Microbalance, FET: Field-Effect-Transistor, NA: not available).

Table 6. Summary of methods used for the detection of MMPs.